Distributed Control Strategy for Low-Voltage Three-Phase Four-Wire Microgrids: Consensus Power-Based Control

Daniele M. Ferreira, Danilo I. Brandao, *Member, IEEE,* Gilbert Bergna-Diaz, *Member, IEEE,* Elisabetta Tedeschi, *Senior Member, IEEE,* and Sidelmo M. Silva, *Member, IEEE*

***Abstract*—Most of the distributed control strategies for grid-connected power converters are droop-based approaches composed of converters driven in voltage-control mode, based on local and shared data with adjacent units. They are usually combined with consensus protocols to deal with the trade-off between power sharing accuracy and voltage/frequency regulation. To achieve the desired results these control systems usually incorporate other techniques and need to take into account details of primary control dynamic. Additionally, power flow control and current unbalance compensation at the PCC are rarely addressed in such approaches. Contrariwise, the centralized control strategy power-based control has been successful in achieving these functionalities. It is oriented to a set point selection to the whole system, considering converters driven in current-control mode and a central converter in voltage-control mode. However, the dependence on centralized communication network in this method still requires improvement. Thereby, the complementary features of both strategies are combined herein in the consensus power-based control, based on a master/slave peer-to-peer integration using sparse communication. This model-free approach provides all aforementioned benefits to the grid without any other technique. Implementation complexity and costs are decreased, while the flexibility and reliability are enhanced. All these achievements are demonstrated by simulation results under different operational conditions and compared to previous works.**

***Index Terms*—Distributed control, consensus protocol, master/slave, microgrids, peer-to-peer, power-based control, power sharing.**

I. Introduction

THE traditional centralized power systems have experienced extensive changes in the last decades. Most of them are associated with the high penetration of renewable-based distributed generators (DGs), as a sustainable way to supply the growth in load demand. In this context, the need of interconnection of these DGs with the preexisting components in the power system, as well as enhanced system reliability and economical benefits, have promoted the microgrid (MG) model as a promising solution to the future of electrical grids [1]. However, to fully exploit their benefits, achieving safe operation, as well as satisfactory power quality in both MG operating modes, i.e. grid-connected (GC) and islanded (IS), there are still challenges to overcome. Among them, the proper coordinated control of converters spread over the MG is crucial for its progress [2].

The communication network (NT), i.e., information and communication technology (ICT), necessary for the control operation, is normally classified into: *i)* decentralized, *ii)* distributed, and *iii)* centralized architectures. Each approach leads to different benefits to the MG as well as to specific challenges.

The decentralized methods are communication-free approaches. Most of the proposals are based on $V-f$ control of converters in voltage-control mode, in which the power sharing is related to the droop coefficients. Despite the contributions achieved in this field, there are still challenges [3], such as: trade-off between the accuracy of power sharing and voltage/frequency regulation; slow dynamics due to the low-pass filter; model-based approaches might be required; and grid power flow control and current unbalance compensation at the MG point of common coupling (PCC) are rarely addressed. The main advantages are scalability and robustness against communication failures.

An appealing solution to minimize some of the listed problems but keeping most advantages of decentralized approaches is the adoption of strategies based on cooperative multi-agent systems, which commonly associate the droop control with the *consensus protocol* [4]. Despite the need of communication, these approaches are based on sparse NT and offers flexibility in terms of communication topology organization. The distributed communication NT represents an interesting intermediate solution for most of the features. The consensus protocol stands out as a flexible technique, suitable to be combined with other strategies and to achieve different objectives, which has provided important contributions in the last years. Some of the most important related works are presented and summarized in the following.

A. Previous works - literature review

The adoption of consensus protocol offers flexibility to develop the control strategy according to the project priorities, e.g., cost reduction, increase of reliability, power sharing accuracy, etc. The methods summarized in Fig. 1, [5], [6], [7], [8], [9], [10], [11], [12], [13], [14], [15] and

D. Ferreira, S. Silva and D. Brandao are with the Graduate Program in Electrical Engineering, Federal University of Minas Gerais, Belo Horizonte, Brazil e-mail: (danielemf@eng-ele.dout.ufmg.br).

G. Bergna-Diaz is with the Department of Electric Power Engineering, Norwegian University of Science and Technology, Trondheim, Norway.

E. Tedeschi is with the Department of Electric Power Engineering, Norwegian University of Science and Technology, Trondheim, Norway and also with the Department of Industrial Engineering, University of Trento, Trento, Italy.

Manuscript received Xxxx XX, XXXX; revised Xxxxx XX, XXXX.

	MAIN FEATURES	REFERENCES																
		[5]	[6]	[7]	[8]	[9]	[10]	[11]	[12]	[13]	[14]	[15]	[16]	[17]	[18]	[19]	[20]	THIS PAPER
		2015	2015	2015	2016	2017	2018	2018	2018	2018	2019	2019	2019	2018	2018	2019	2019	2020
GENERAL INFORMATION	Microgrid type	AC MG	AC MG	AC MG	AC MG	AC MG	AC MG	AC MG	AC MG	AC MG	AC MG	DC MG	AC/DC MGC	AC MG	AC MG	AC MG	AC MG	AC MG
	Operation mode of interest	IS	IS	IS	IS	GC	GC	GC, IS, TR	IS	IS	IS	IS	GC	GC, IS	IS	GC, IS, TR	GC	GC, IS, TR
	Strategies and techniques adopted	AVGC OPT OTHERS	AVGC LFC DROOP	AVGC DROOP	AVGC DROOP VIRT	LFC	AVGC LFC DROOP VIRT OTHERS	LFC DROOP	LFC DROOP OTHERS	AVGC DROOP OTHERS	AVGC OTHERS	LFC DROOP VIRT	AVGC LFC DROOP VIRT	DROOP	DROOP VIRT OTHERS	PBC	DROOP	LFC PBC
STRATEGY'S ACHVIEMENTS	Accurate active power sharing	DGs costs	droop	droop	droop	DGs capacity	droop	droop	droop	DGs costs	DGs capacity	droop	droop	droop	droop	DGs capacity	droop	DGs capacity
	Accurate reactive power sharing	DGs costs	droop	droop	DGs capacity	DGs capacity	droop	droop	-	droop	-	-	droop	no	droop	DGs capacity	droop	DGs capacity
	Accurate frequency	yes	yes	yes	yes	-	yes	yes	yes	yes	yes	yes	yes	yes	yes	yes	yes	yes
	Accurate voltage	yes	yes	yes	yes	yes	yes	yes	-	yes	yes	yes	yes	yes	yes	yes	yes	yes
	Unbalance compensation	no	no	no	yes	no	yes	no	-	no	no	no	yes	yes	yes	yes	yes	yes
	Harmonic compensation	no	no	no	yes	no	no	no	-	no	no	no	yes	no	yes	no	-	no
	Control of power flow at PCC	no	no	no	no	yes	no	yes	-	no	no	no	yes	yes	yes	yes	no	yes
SCENARIOS ADRESSED IN THE RESULTS	Behaviour under communication failure	no	yes	no	yes	no	no	yes	no	yes	no	yes	yes	no	no	no	no	yes
	Behaviour under time-delay	no	no	no	yes	no	no	no	yes	no	no	yes	yes	no	no	yes	no	yes
	Behaviour under agent's failure	no	no	no	no	no	no	yes	no	no	no	yes	yes	no	no	no	yes	yes
	Implementation with DGs in different power ratings	yes	yes	yes	no	no	yes	-	yes	yes	yes	yes	yes	yes	no	yes	no	yes
	Plug-and-play capability	yes	yes	no	yes	yes	yes	yes	no	yes	no	yes	yes	no	no	yes	no	yes

Fig. 1. Comparative summary of the literature review - Main achievements and limitations.

[16], are examples of important efforts from 2015 to 2020 for the MGs development. They are compared according to specific features of the proposals, in order to provide an overview of the progress already achieved in this segment and the existing challenges to be overcome. Even without applying any consensus protocol or concept of cooperative multi-agent systems, the works [17], [18], [19] and [20] are also included due to their relevant features for the proposal herein.

In the presented summary the references are compared in terms of the applications (AC and DC MGs, and also the called MGs clusters (MGC)), operation mode of interest (IS, GC, and transitions between different modes), and the methods/techniques adopted in the control system development (average-consensus protocol (AVGC), leader-follower consensus protocol (LFC), optimization technique (OPT), droop control (DROOP), virtual impedance method (VIRT), power-based control (PBC), etc). The main achievements of the control system proposed in each work are also highlighted, followed by the operating conditions explored in the results available in the related manuscripts.

As can be seen in Fig. 1, most of these efforts from the last years are still focused on the achievement of accurate power sharing and voltage/frequency regulation by a feasible and reliable control, as [6], [11], [12], [13], [15], [17], [18], [19], [20], as well as [7], [8], [10] and [14], which are specially dedicated to solve the trade-off between reactive power and voltage regulation. Besides the power sharing, unbalance and/or harmonic compensation are also achieved by [8], [18] and [19]. The power sharing of energy storage systems is explored by [9] in order to avoid power fluctuation at PCC, and a cost optimization for load shedding is proposed in [5].

From the 16 references covered in Fig. 1, 12 apply the concept of cooperative multi-agent systems and consensus theory in the development of the proposed control strategy. From these 12 works, 9 combine the consensus protocol with the droop control, usually achieving the power sharing proportional to the droop coefficients. Few of them achieve the power flow control or unbalance compensation at PCC or addresses the main operational conditions in the presented results. The summary of Fig. 1 evidences important progress and valuable achievements in the control system development for MGs. However, each proposal is focused on specific priorities and a compromise among different objectives may be still considered as a challenge.

B. Motivation

To overcome the aforementioned challenges providing a robust, feasible and flexible control system, many modified droop techniques emerged in this segment, e.g., associated with virtual impedance-based methods [8], trying to promote accurate power sharing without communication. However, despite the benefit of a communication-free approach, these methods are usually combined with other techniques, aggregating complexities to the control systems. In addition, distributed methods based on consensus protocols are usually designed taking into account details of the DGs' primary control, such as converter dynamics, current-control and phase-locked loop, also increasing the method complexity, e.g., the strategy distributed-averaging proportional–integral (DAPI) proposed in [6], mainly focused on voltage/frequency regulation.

Whereas the power sharing still deserves attention in decentralized and distributed approaches, this is the main feature offered by the centralized control strategy *power-based control* (PBC). The PBC, originally proposed in [21], offers accurate power sharing proportional to the DGs available capability, power flow control and current unbalance compensation at

PCC. It is based on the set point selection to the whole system, without previous knowledge of MG parameters and through simple algebraic formulation. Satisfactory results have been achieved with this strategy in stable operation under different scenarios [22], [23]. Nevertheless, there is still the undesired dependence on a centralized communication NT for its operation, which affects the MG scalability, reliability, flexibility of the communication topology, and related costs.

C. Contributions

Considering the gaps identified in the previous works and the complementary features of the consensus-based control and the PBC, both are combined herein in the *Consensus Power-Based Control* (Consensus-PBC) for low-voltage three-phase four-wire MGs. This approach is based on master/slave peer-to-peer integration using sparse communication NT considering a MG structure comprised of DGs (single- and/or three-phase) in current-control mode and a central three-phase converter in voltage-control mode.

It is important to highlight that, although the proposed strategy does not present specific limitations for implementation in different types of MGs, this paper focuses on its application on urban MGs. In this kind of application the power system is more homogeneous in terms of geographical distribution of loads, and DGs are separated by short distances. In such condition, the proportional power sharing may achieve quasi-optimal results [24]. This paper aims at minimizing challenges of the techniques involved, while better exploiting their benefits. Thus, the achievements of the proposal in this manuscript are discussed in the following.

- Contributions to the NT:
  - *i)* Accurate active and reactive power sharing proportional to the DGs available capabilities;
  - *ii)* Accurate active and reactive grid power flow control among different phases of the MG;
  - *iii)* Current unbalance compensation at PCC.

The contributions claimed above are not novel if individually analyzed, since other works had already provided one or more of these benefits, e.g., the original PBC [22]. However, as evidenced in Fig. 1, few distributed strategies based on consensus protocol are able to provide all listed benefits at the same time, keeping low complexity of the algorithm, communication flexibility and satisfactory performance in different operational conditions.

Additionally, due to the scientific maturity of the consensus protocol technique, there is a vast amount of literature applied to different practical disciplines, as well as theoretically-oriented results focusing on its mathematical formulation. On the one hand, this rich legacy may offer many benefits for a relatively new application such as MGs. On the other hand, the wide range of technical content available from different scientific fields may complicate the task of collecting the fundamental concepts about this technique, which are in turn necessary for its successful application to, and steady development of MGs.

Besides the achievements that have been commonly sought by researchers in this segment–denominated above as contributions to the NT–the paper herein offers also a theoretical contribution to consensus-based control approaches in general.

- Theoretical contribution to consensus-based strategies:
  - *i)* General steady-state and stability analysis for leader-follower consensus protocol in discrete-time, considering a linear system with first-order integral, based on the system eigenvalues features.

Apart from the contributions presented, some positive features also resulted from the methods combination adopted, which can enhance the control system feasibility in MGs applications.

- Special features of Consensus-PBC:
  - *i)* Model-free implementation, independent of detailed grid parameters and no need of parameters tuning. Detailed system dynamic and/or additional methods are not necessary, such as virtual impedance techniques, sequence component decomposition, etc., keeping low complexity formulation;
  - *ii)* Suitable for any DG primary control, since it operates in current-control mode;
  - *iii)* Suitable for single-phase converters arbitrarily connected (i.e., line-to-neutral or line-to-line)–a relevant feature in the Brazilian distribution system–as well as three-phase converters;
  - *iv)* Enhancement of MG scalability due to the distributed communication topology;
  - *v)* Enhancement of flexibility to choose a communication topology according to the project priorities;
  - *vi)* Satisfactory results under general operational conditions, such as communication failures, communication time-delays, agent's failures, different agents' power rating and during plug-and-play process;
  - *vii)* Satisfactory reliability depending on the communication topology.

The paper is organized as follows: Section II describes the MG structure and related control organization; Section III covers the consensus-based control and PBC; Section IV proposes the Consensus-PBC; Section V presents simulation results, Section VI provides a comparison of the results with other proposals from the literature, and Section VII concludes.

II. MG Structure and Control Organization

The unbalanced low-voltage 43-nodes MG in Fig. 2 is the structure considered herein. The system is composed of five active nodes in phase a, three in phase b, and four in phase c, where the single-phase i^{th} DGs, $i \in \{1, 2, 3, ..., n\}$, are arbitrarily connected, besides of three active nodes of three-phase DGs. All DGs operate in current-control mode in both MG operation modes. A three-phase central converter called utility interface (UI), sited at the MG PCC, guarantees IS operation and smooth transitions from and to GC operating mode. It is equipped with ES and operates as a grid-forming converter to the whole MG. The DGs are coordinately driven by a master controller (MC), usually implemented in the UI.

The control architecture is organized in three different levels: primary, secondary, and tertiary control. The primary level is performed at the DGs' local controllers and covers their basic functions for a proper operation without relying

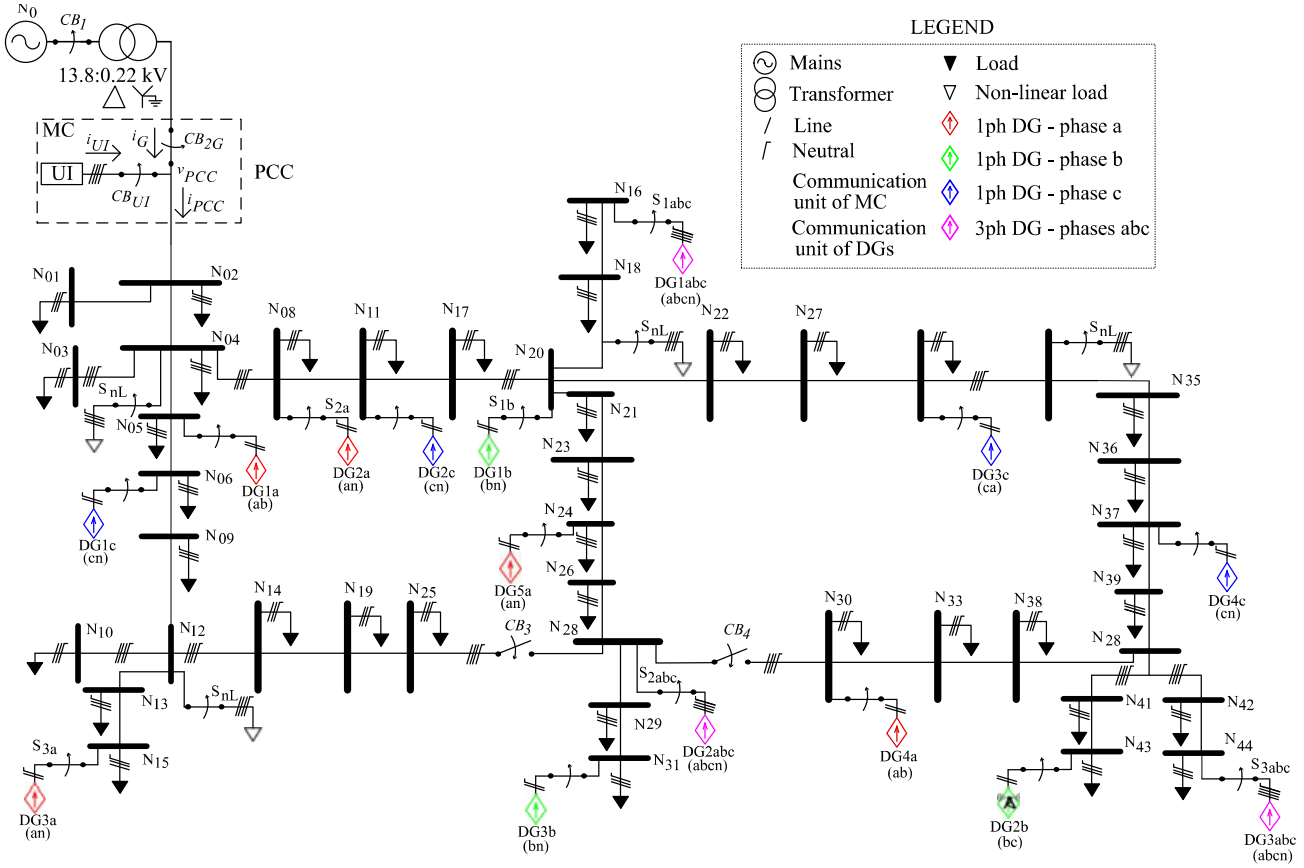

Fig. 2. Three-phase four-wire microgrid structure considered.

on communication. The secondary level, focus herein, is also performed at the DGs' local controller but is related to the management of the MG resources and its operation is dictated by the MC through sparse communication. The tertiary level is responsible for the interaction between the MG and the main grid (i.e., Distribution System Operator (DSO)). The adopted sparse communication NT is based on a peer-to-peer infrastructure and the topologies are presented in Section IV.

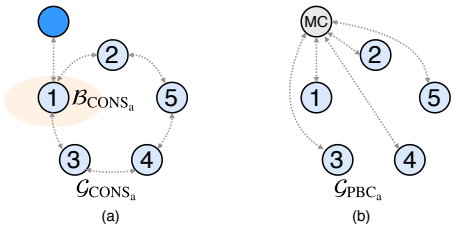

Fig. 3. MG graphs for (a) consensus-based control, (b) power-based control.

III. Fundamentals of Consensus-Based and Power-Based Control

A. Consensus-Based Control

The graph $\mathcal{G}_{\text{CONS}_a}$ shown in Fig. 3(a) for phase a of the MG considered herein represents a typical communication NT based on consensus protocol–for a detailed tutorial on graph theory refer to [25]. In this architecture the primary and secondary control levels are implemented at each DG and the local information are transmitted among adjacent units in order to reach a consensus.

This agreement depends either on the agent's initial states, called *average-consensus problem*, usually without the root node highlighted in Fig. 3(a)–see formulation in [26]–or on external signals dictated by the root node, called *leader-following problem*, in which the formulation considers a linear system with first-order integral as in (1)

$$x_i(l+1) = x_i(l) + \epsilon[\sum_{j=1}^{n} a_{ij}(x_j(l) - x_i(l)) + \\ + b_{ii}(x^{\text{ref}}(l) - x_i(l))], \tag{1}$$

where n is the total of active agents in the system represented by the vertices in $\mathcal{G}_{\text{CONS}_a}$, a_{ij} is the adjacency between the nodes i and $j \in \{1, 2, 3, ..., n\}$, and $n_{a_{ij}}$ is the total of neighbors directly connected. $\mathcal{B}_{\text{CONS}_a}$ is a subgraph of $\mathcal{G}_{\text{CONS}_a}$ with the vertices directly connected to the leader node. Thus, $b_{ii} = 1$ if $i \in \mathcal{B}_{\text{CONS}_a}$ and $b_{ii} = 0$ if $i \notin \mathcal{B}_{\text{CONS}_a}$. The variables x_i and x_j are the agents' local states for i and j, at a specific iteration l and step-size ϵ bounded by (3). The constrain imposed by the leader node is x^{ref}.

The formulation in (1) is written in matrix notation as

$$\boldsymbol{x}(l+1) = \mathcal{P}\boldsymbol{x}(l) + \epsilon\boldsymbol{B}[\boldsymbol{x}^{\text{ref}}(l) - \boldsymbol{x}(l)], \tag{2}$$

where $\mathcal{P} = \mathbb{I} - \epsilon\mathcal{L}$ is the Perron matrix $\mathcal{P} \in \mathbb{R}^{n\times n}$ and $\mathcal{L} = \mathcal{D} - \mathcal{A}$ is the Laplacian matrix $\mathcal{L} \in \mathbb{R}^{n\times n}$ defined in [26]. The matrices $\mathcal{D} \in \mathbb{R}^{n\times n}$ and $\mathcal{A} \in \mathbb{R}^{n\times n}$ are the degree and adjacency matrices, respectively. The matrix $\boldsymbol{B} \in \ltimes^{n\times n}$ is diagonal with the elements b_{ii} and $\boldsymbol{x} \in \mathbb{R}^n$ is the vector related to the states of the agents $\boldsymbol{x}(l) = [x_i(l), x_j(l), ...x_n(l)]^\top$.

$$0 < \epsilon < 1/\Delta_{\mathcal{D}+\boldsymbol{B}}, \tag{3}$$

In (3), $\Delta_{\mathcal{D}+\boldsymbol{B}}$ is the maximum value of the sum $\mathcal{D}+\boldsymbol{B}$. The consensus is achieved in this system if all elements represented by vertices in $\mathcal{G}_{\text{CONS}_\text{a}}$ have converged to the same value, i.e., $\boldsymbol{x}(l) = [\alpha, ..., \alpha]^\top = \alpha\mathbf{1}$ and $\alpha \in \mathbb{R}^n$. In general, most of the contributions from the literature applying consensus protocols in MGs are widely combined with the droop control, e.g., [13], as previously discussed.

B. Power-Based Control

The PBC strategy is established on a fully centralized communication topology [22]. The PBC is implemented in the MC and acts at the secondary level of the control organization previously described in Section II. It does not rely on synchronization algorithm, since the DGs in this approach in current-control mode, following the voltage and frequency at their corresponding point of connection. However, the heterogeneous operation considering current- and voltage-control mode in PBC-MG has been also investigated in [23]. Moreover, the voltage-control mode DGs in the AC side can be power-controlled by considering droop-control as in [27], or voltage-driven with the triple-loop control as in [28]. Applying one of these control methods, the power demand during transient can be shared among the DGs controlled as voltage-source and the UI converter itself.

The PBC is able to manage the operation of single-phase DGs, as proposed in [22], as well as three-phase DGs according to the newest PBC generation presented in [23]. The proposal herein adopts the method in [23], where three-phase DGs operates coexisting in the NT with single-phase DGs, arbitrarily connected (phase-to-line and phase-to-phase).

The PBC performs the power sharing remotely driving the DGs according to signal commands α_P and α_Q. A scaling coefficient per phase is calculated to promote active (α_{P_a}, α_{P_b}, α_{P_c} in (4)) and reactive (α_{Q_a}, α_{Q_b}, α_{Q_c} in (5)) power sharing and unbalance compensation. Other scaling coefficient for the three-phases is calculated to manage the three-phase DGs ($\alpha_{P_{abc}}$ as in (6) and $\alpha_{Q_{abc}}$ shown in (7)), which operates balanced in the active and reactive power sharing.

The scaling coefficients are broadcasted by the MC to each DG_i through the ICT [21], [22]. During each control cycle l the scaling coefficients α_P and α_Q steer the proportional active and reactive contribution of each DG_i based on the MG demand. This demand is estimated based on the data packet information sent by each active node i in the previous cycle, on measurements of P_G, Q_G, P_{UI}, Q_{UI}, and the polarity signs defined in Fig. 2.

$$\alpha_{P_{1\phi}}(l+1) = \frac{P_G(l) + P_{UI}(l) + \sum_1^{n_{1\phi}} P_i(l) - P_G^*(l+1)}{\sum_1^{n_{1\phi}} P_{max_i}(l)}, \tag{4}$$

$$\alpha_{Q_{1\phi}}(l+1) = \frac{Q_G(l) + Q_{UI}(l) + \sum_1^{n_{1\phi}} Q_i(l) - Q_G^*(l+1)}{\sqrt{\sum_1^{n_{1\phi}} A_{inv_i}(l)^2 - \sum_1^{n_{1\phi}} P_i(l)^2}}, \tag{5}$$

$$\alpha_{P_{3\phi}}(l+1) = \frac{P_G(l) + P_{UI}(l) + \sum_1^{n_{1\phi,3\phi}} P_i(l) - P_G^*(l+1)}{\sum_1^{n_{1\phi,3\phi}} P_{max_i}(l)}, \tag{6}$$

$$\alpha_{Q_{3\phi}}(l+1) = \frac{Q_G(l) + Q_{UI}(l) + \sum_1^{n_{1\phi,3\phi}} Q_i(l) - Q_G^*(l+1)}{\sqrt{\sum_1^{n_{1\phi,3\phi}} A_{inv_i}(l)^2 - \sum_1^{n_{1\phi,3\phi}} P_i(l)^2}}, \tag{7}$$

where P_G and Q_G are the active and reactive power provided by the main grid, P_{UI} and Q_{UI} are the power contribution of the central converter, P_i and Q_i are the power contribution of each DG_i. The quantities P_G^* Q_G^* are the grid power references to dispatch the MG. P_{max_i} and A_{inv_i} are the maximum active power available and the converter rated power of each DG_i, respectively. These quantities may be single-phase or three-phase, depending on the scaling coefficient to be calculated, considering $n_{1\phi}$ only the single-phase converters and $n_{1\phi,3\phi}$ both single- and three-phase converters. The complete PBC formulation is found in [23].

IV. Consensus Power-Based Control

The Consensus-PBC does not need a detailed MG model (i.e., line impedances and topology), and unlike many consensus approaches in MG applications, the protocol is designed without taking into account details of the primary control (i.e., converter dynamics, current-control, phase lock loop, etc), which commonly add complexities to the formulation, such as higher-order integrator dynamics and non-linearity. Thus, the protocol design is limited to the information exchange dynamics among units, which can be easily represented by means of a first-order integral update law. The states of interest are only the scaling coefficients presented in (4)-(7). This simplifies the formulation of the leader-following consensus problem as shown in (1). The leader acts at the PCC, regulating the grid power flow into the upstream power system, which is main reason for adoption of the leader-follower consensus protocol instead the average consensus protocol, as in many works found in the literature. Additional methods, e.g., optimization algorithms, sequence decomposition, virtual impedance, droop control, are not necessary to achieve the contributions discussed in Section I-C.

A. Microgrid Structure

The Consensus-PBC is developed considering the MG structure of Fig. 2 with the sparse communication topology of

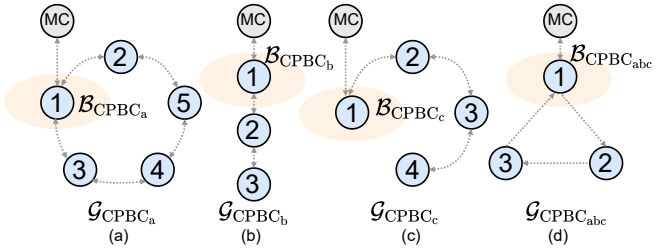

Fig. 4. Graphs for Consensus-PBC: (a) DGs at phase *a*, (b) DGs at phase *b*, (c) DGs at phase *c* and (d) three-phase DGs at phases *abc*.

Fig. 4. Each phase is considered individually for the single-phase converters in order to promote the unbalance compensation besides active and reactive power sharing (please refer to Section III-B). The communication links may assume different topologies, as long as the stability conditions described in Subsection IV-C are attained. Herein the related graphs are differently and arbitrarily chosen, only to demonstrate the method flexibility and how this choice might be managed according to the project priorities, e.g., to enhance MG feasibility.

In general, the communication interconnects each DG_i to its neighbors and the MC to at least one of the generation unit per phase. Each unit may be both client and server. The communication links are based on low data transfer speed (i.e., up to few hundreds of kbps) and low-bandwidth (i.e., 9600 to 115200 bps) technology. The MC processes all related information computing the scaling coefficients as a leader node of the multi-agent system, as shown by the root node in Fig. 4.

As previously described for the PBC in Subsection III-B, the UI is a key element to ensure the MG IS operation, providing the voltage/frequency references to all DGs that operate in current-control mode. Observe that in this considered structure, there is the possibility to overload the UI converter if substantial load is connected to the AC bus. However, this issue has already been solved by using droop scheme in AC grid and is not going to be addressed in details herein. Although voltage-control converter are not considered in the the case studies covered in this paper, they could be also accommodated in such proposed MG control [27], [28].

B. Implementation of Consensus Power-Based Control

To steer all the DGs to the same scaling coefficients computed by the leader node (i.e., MC) the Consensus-PBC strategy follows the steps shown in the flow chart of Fig. 5. The low complexity of this method is a feature to be highlighted. Two information previously defined are necessary for the algorithm steps: *i)* the maximum number of DGs allowed to be installed in each phase and, *ii)* an individual identifier number for each DG. For phase *a* in Fig. 4 both parameters are $n_a = 5$ and $i_a = 1,\ 2,\ 3,\ 4,\ 5$. This information is used for the construction of matrix ($\mathbf{M}_{\mathbf{IF}_{P_{MG_{DG_i}}}}$) and vectors ($\mathbf{v}_{\mathbf{IF}_{P_{MG_{DG_i}}}}$) structures necessary to allocate the data exchanged in the distributed NT.

In urban MG, focus of this manuscript, n may be defined in the MG project stage and it is based on the capacity of the communication infrastructure adopted. This sizing may be also associated to the MG hosting capacity [29], also defined in the initial stages of the MG implementation. The other parameter i may be attributed to the DG installation when the power supplier allows the connection of the distributed system to the grid. Once both information are registered in the control system algorithm, later additional changes are not necessary for the control strategy operation and the MG plug-and-play capability is ensured (covered in detail in V-B3). The flow chart steps illustrated in Fig. 5 are described as follows.

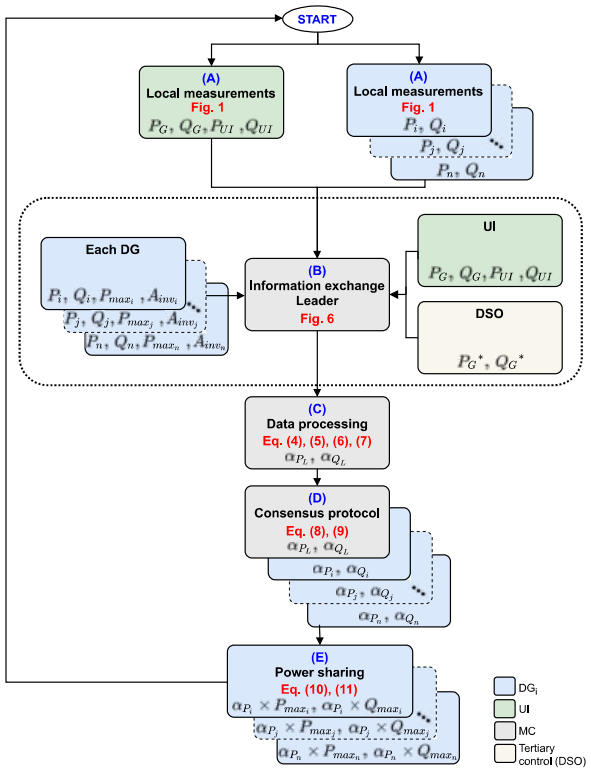

Fig. 5. Flow chart implementation of the proposed Consensus-PBC.

1) Local Measurements: first of all, the quantities for the calculation of (4)-(7) are measured locally by the converters in each control cycle l, as follows: considering Fig. 2, $P_{UI}(l)$ and $Q_{UI}(l)$ are measured at the UI output; $P_G(l)$ and $Q_G(l)$ are measured at the grid side of the PCC; and $P_i(l)$ and $Q_i(l)$ are measured at the output of each DG_i. The nominal quantities $P_{max_i}(l)$ and $A_{inv_i}(l)$ are also sent by DG_i to the MC according to their individual capabilities.

2) Information Exchange: the target in this step is to convey all quantities described in the previous stage to the MC through the sparse NT available. The variables measured, i.e., $P_G(l)$, $Q_G(l)$, $P_{UI}(l)$, and $Q_{UI}(l)$, are directly sent to the MC. For the other variables the procedure is shown in Fig. 6, considering the graph of phase *a*. Such procedure is applied individually to each quantity that has to be exchanged by each DG_i: $P_i(l)$, $Q_i(l)$, $P_{max_i}(l)$, and $A_{inv_i}(l)$. In the proposed method, the information is exchanged among the neighbor agents through a data packet allocated in a vector $\boldsymbol{v_{IF}} \in \mathbb{R}^n$. That means, in each edge (link between two agents) flows a data packet with $four$ variables $\times$ n number of DGs.

The data from each DG_i is allocated in the vector $\boldsymbol{v_{IF_i}}$ in

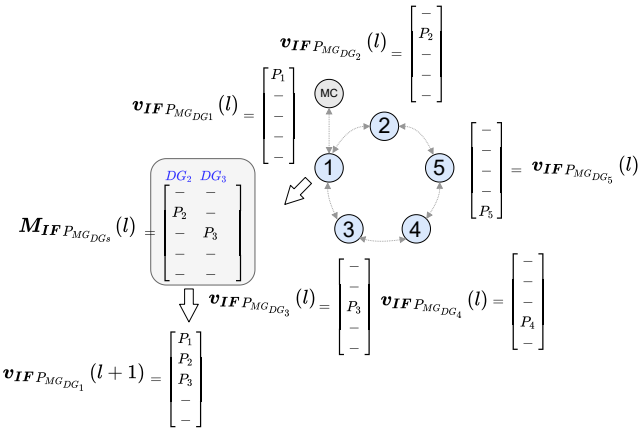

Fig. 6. Information exchange (i.e., step (B)) for Consensus-PBC.

the row corresponding to the related identifier number i. This vector is shared among adjacent agents and is processed in the receiver agent placed in a matrix $\boldsymbol{M_{IF}} \in \mathbb{R}^{n \times n_{a_{ij}}}$ at the column i. In the filled out matrix (see $\boldsymbol{M_{IF}}_{P_{MG_{DGs}}}$ in Fig. 6), the values received are compared with each other, column to column. The quantity values regarding adjacent agents just replace the old ones in the updated vector $l+1$. Whether the agent receives data regarding agents that are not adjacent (indirectly by the adjacent units), there are two possibilities: *(1)* all adjacent agents inform the same value, this value is placed in the updated vector $l+1$; *(2)* the adjacent agents inform different values regarding the same DG, the average of the values available is placed in the updated vector.

3) Data Processing: once all information has reached the MC, the total demand of the MG is estimated considering $[P_G(l)+P_{UI}(l)+\sum_1^n P_i(l)]$ and $[Q_G(l)+Q_{UI}(l)+\sum_1^n Q_i(l)]$, and also the total power available in the system $[\sum_1^n P_{max_i}(l)]$ in the current control cycle, l. Considering the information from the tertiary control (normally set by DSO), P_G^* and Q_G^*, the power flow at the PCC is regulated subtracting this power amount of the MG demand, as in the numerators of (4)-(7). With the information collected, the scaling coefficients are phase-dependent computed for the single-phase converters ($\alpha_{P_{L_a}}$, $\alpha_{P_{L_b}}$, $\alpha_{P_{L_c}}$) and ($\alpha_{Q_{L_a}}$, $\alpha_{Q_{L_b}}$, $\alpha_{Q_{L_c}}$), applying (4) and (5), and other scaling coefficient common to the three phases are computed for the three-phase DGs ($\alpha_{P_{L_{abc}}}$, $\alpha_{Q_{L_{abc}}}$) by the leader (L), as in (6) and (7), respectively.

4) Consensus Protocol: to converge all the DGs to the same α_P and α_Q, these variables are then the states in the multi-agent system, which are led by the MC to achieve proportional power sharing and steer grid power flow. The consensus protocol is devised by (1) in each DG_i resulting in (8) and (9). The agents that receive the information directly from the leader (MC) belong to the subgraph called $\mathcal{B}_{\mathrm{CPBC_{ph}}}$, highlighted in the graphs of Fig. 4. The convergence conditions are presented in Subsection IV-C.

$$\alpha_{P_i}(l+1) = \alpha_{P_i}(l) + \epsilon \sum_{j=1}^{n} a_{ij}(\alpha_{P_j}(l) - \alpha_{P_i}(l) + b_i\big(\alpha_{P_L}(l) - \alpha_{P_i}(l)\big)\big), \tag{8}$$

$$\alpha_{Q_i}(l+1) = \alpha_{Q_i}(l) + \epsilon \sum_{j=1}^{n} a_{ij}(\alpha_{Q_j}(l) - \alpha_{Q_i}(l) + b_i\big(\alpha_{Q_L}(l) - \alpha_{Q_i}(l)\big)\big), \tag{9}$$

5) Local Generation: considering that the convergence has been achieved in the system during step (D), the local controllers of DGs set the active and reactive power, P_i^* and Q_i^* applying (10) and (11), respectively:

$$P_i^* = \alpha_P(l+1) \cdot P_{max_i}, \tag{10}$$

$$Q_i^* = \alpha_Q(l+1) \cdot Q_{max_i}, \tag{11}$$

where $Q_{max_i} = \sqrt{A_{inv_i}^2 - P_i^2}$. The scaling coefficients are percentage quantities and therefore the power contribution of each DG_i to the MG is proportional to its available capability.

C. Steady-State and Stability Conditions

1) Analysis for Ideal Communication Structure: the convergence of the proposed strategy is achieved if the individual information regarding each DG reaches the MC (i.e., step (B) - information exchange) and if the DG's states converge to the same scaling coefficients sent by the MC (i.e., step (D) - consensus protocol).

The necessary condition to guarantee the information exchange is to have a path connecting each node to any other node in the system, i.e., a strongly connected graph (SCG). In turn, considering the point $\tilde{x} = x - x^\star$, where $x^\star$ is the equilibrium point of interest, the steady-state and stability of the leader-following consensus protocol in discrete-time in (8) and (9) may be analyzed as following.

Steady-State Analysis: for the steady-state analysis and the value of convergence, it is considered the relation

$$\boldsymbol{x}^\star(l+1) - \boldsymbol{x}^\star(l) = -\epsilon \mathcal{L}\boldsymbol{x}^\star(l) - \epsilon \boldsymbol{B}\boldsymbol{x}^\star(l) + \epsilon \boldsymbol{B}\boldsymbol{x}^{\mathrm{ref}}(l). \tag{12}$$

If $\boldsymbol{x}^\star(l+1) - \boldsymbol{x}^\star(l) = 0$, thus

$$\mathcal{L}\boldsymbol{x}^\star(l) + \boldsymbol{B}\boldsymbol{x}^\star(l) = \boldsymbol{B}\boldsymbol{x}^{\mathrm{ref}}(l). \tag{13}$$

Since the Laplacian matrices have a left eigenvector $\gamma \in \mathbb{R}^n$, (13) may be written as

$$\boldsymbol{\gamma}^\top \mathcal{L}\boldsymbol{x}^\star(l) + \boldsymbol{\gamma}^\top \boldsymbol{B}\boldsymbol{x}^\star(l) = \boldsymbol{\gamma}^\top \boldsymbol{B}\boldsymbol{x}^{\mathrm{ref}}(l),$$

Considering that this left eigenvector γ is associated to the trivial eigenvalue $\lambda_1 = 0$, $\gamma^\top \mathcal{L} = 0$ [26], and that there is just one agent receiving the information directly from the leader, as in the graphs herein, just one term in the diagonal of the

matrix $\boldsymbol{B}$ is equal to one and the other elements are equal to zero, which leads to $\boldsymbol{B}\boldsymbol{x}^{\star}(l) = \boldsymbol{B}\boldsymbol{x}^{\mathrm{ref}}(l)$. Replacing it in (13)

$$\begin{aligned} \mathcal{L}\boldsymbol{x}^{\star}(l) + \boldsymbol{B}\boldsymbol{x}^{\mathrm{ref}}(l) =& \boldsymbol{B}\boldsymbol{x}^{\mathrm{ref}}(l), \\ \mathcal{L}\boldsymbol{x}^{\star} =& \, 0. \end{aligned} \tag{14}$$

As the sum of each row in $\mathcal{L}$ is always zero, 0 is a trivial eigenvalue ($\lambda_1 = 0$) of the related Laplacian matrix and it is associated to the right eigenvector $\mathbf{1} \in \mathbb{R}^n$ [26]. Thus, to ensure (14), all states have to achieve the same value. If the agent associated to $b_{ii} = 1$ is equal to the value dictated by the leader node, therefore all agents have achieved the same value $\boldsymbol{x}^{\star}(l) = \boldsymbol{x}^{\mathrm{ref}}$.

Stability Analysis: the leader-following consensus problem in discrete-time may be rewritten as in (15):

$$\begin{aligned} \tilde{\boldsymbol{x}}(l+1) - \tilde{\boldsymbol{x}}(l) =& -\epsilon\mathcal{L}\tilde{\boldsymbol{x}}(l) - \epsilon\boldsymbol{B}\tilde{\boldsymbol{x}}(l), \\ =& (\mathcal{P} - \epsilon\boldsymbol{B})\tilde{\boldsymbol{x}}(l), \end{aligned} \tag{15}$$

where $(\mathcal{P} - \epsilon\boldsymbol{B}) = \boldsymbol{Q}$, $\boldsymbol{Q} \in \mathbb{R}^{n\times n}$.

Considering the system described by $\boldsymbol{x}(l+1) = \boldsymbol{Q}\boldsymbol{x}(l)$ and its eigenvalues by λ_i, the stability is verified if the *Perron-Frobenius* Theorem [30] is attained and if the eigenvalues of $\boldsymbol{Q}$ lie inside the unit circle of the *Gershgorin* disks [31]. A practical way to verify it is to analyse whether the matrix $\boldsymbol{Q}$ is irreducible (graph strongly connected) [32], non-negative ($q_{ij} \geq 0$) [33], primitive (a single λ_i with maximum modulus) [34] and row-stochastic (maximum —λ_i|=1, i.e., inside the unit circle) [34].

For the sake of space, the properties of the Perron matrix are not shown in details herein, but all these conditions are satisfied according to [26]. Since the characteristics of the Perron matrix it is known, it is necessary to analyze the effect of the term $\epsilon\boldsymbol{B}$ on the eigenvalues of $\boldsymbol{Q}$, considering that $\boldsymbol{B}$ is a diagonal matrix with ones and zeros. Thus, the relation (15) is expanded as

$$\tilde{\boldsymbol{x}}(l+1) = (\mathbb{I} - \epsilon(\mathcal{L} + \boldsymbol{B}) + \epsilon\mathcal{A})\tilde{\boldsymbol{x}}(l). \tag{16}$$

The Perron matrix of a strongly connected graph is irreducible [26]. Note in (16) that the effect of the term $\epsilon\boldsymbol{B}$ over $\boldsymbol{Q}$ increases the degree of the matrix, according to the number of agents that receive the information directly from the leader. It means that the output matrix $\boldsymbol{Q}$ does not loose connectivity in comparison with the leaderless formulation. Thus, the matrix is still related to a strongly connected graph, and therefore it is still irreducible.

To ensure that $\boldsymbol{Q}$ is non-negative and primitive, the maximum value of the step-size has to be bounded. Observe that, independently of the graph topology, $\mathcal{A}$ is a matrix with non-negative entries, which means that, since $\epsilon > 0$, $\epsilon\mathcal{A}$ is also a matrix with non-negative entries. Thus, the analysis is focused on the other terms $\mathbb{I} - \epsilon\mathcal{D} - \epsilon\boldsymbol{B} \geq 0$. Analyzing element by element, it is necessary to consider the worst case condition of matrix $\mathcal{D}$, its maximum value. Thus, the step-size condition to make $\boldsymbol{Q}$ non-negative is defined such that

$$\begin{aligned} 1 - \epsilon(d_{ii} + b_{ii}) >& \, 0, \\ \epsilon <& \frac{1}{max(d_{ii} + b_{ii})}, \end{aligned}$$

which leads to

$$0 < \epsilon < \frac{1}{\Delta_{\mathcal{D}+\boldsymbol{B}}}. \tag{17}$$

The features analyzed until now ensure that the properties of the *Perron-Frobenius* Theorem hold for the matrix $\boldsymbol{Q}$. Thus, it is also necessary to evaluate if the new eigenvalues still lie inside the unit *Gershgorin* circle. Differently from the average consensus, the row sum equal to one in the Perron matrix is no longer valid for all rows in the matrix $\boldsymbol{Q}$. However, due to the bounded value of ϵ, the $\boldsymbol{Q}$ is affected just on its diagonal. According to *Gershgorin* Theorem, this means that the term $\epsilon\boldsymbol{B}$ changes the centre of the *Gershgorin* disks related to $\boldsymbol{Q}$, keeping the same radius of $\mathcal{P}$.

In short, stability is guaranteed:

- *i)* if the related graph is strongly connected [26], and
- *ii)* since the step-size ϵ is bounded by (3) [35].

2) Stability with Communication Time-Delay and Time-Varying Topology: in parallel to the aforementioned progresses in the field of smart grids, the communication technology has also developed in the last years. This infrastructure is of fundamental importance to promote the functionalities of distributed control systems of MGs. In these communication-based approaches the infrastructure of data transfer needs to handle many challenges involved with smart grids operation and under different conditions. Such challenges differ considerably between wired and wireless solutions, but independent on the adopted technology, this communication NT has to meet some requirements to ensure safe and reliable operation to the electrical NT [36]. IEC 61850 is a relevant international standard to be considered in the design of power communication projects. It provides communication guidelines for the proper operation of DGs integration and the MGs [37], [38].

The first feature to be considered regards the time-delay requirement that the communication NT has to deal with in MG [36] applications. For the control information the standard specifies 100 ms as a general guideline, which despite the considerable evolution in communication technologies may be still challenging.

According to [39], however, the delay in wireless communication in short distances of about 150 m is typically < 500 ns, which could be negligible in application of urban MGs, as is the case herein. Second important feature in communication NT in MGs is the bandwidth limitation covered by [40], [41]. In both references, event-triggered communication mechanisms are presented in order to reduce the communication resource usually necessary for continuous or periodical data transfer. In these methods, it is defined when these piece of information must be transferred without compromising the control stability and performance. A third point to be taken into account is the fact that MGs communication NTs are also very susceptible to noise interference from communication

TABLE I
PARAMETERS OF THE DGS

Parameters	DGs
Identification (i)	[1a, 2a, 3a, 4a, 5a, 1b, 2b, 3b, 1c, 2c, 3c, 4c, 1abc, 2abc, 3abc]
Node	[05, 08, 15, 30, 26, 20, 43, 31, 06, 11, 32, 37, 16, 28, 44]
Connection	[ab, an, an, ab, an, bn, bc, bn, cn, cn, ca, cn, abcn, abcn, abcn]
A_{inv} (kVA)	[3.0, 4.0, 5.0, 5.0, 8.0, 8.0, 8.0, 9.0, 8.0, 5.0, 6.0, 7.0, 10.0, 10.0, 14.0]
P_{max} (kW)	[2.0, 3.0, 4.0, 4.0, 7.0, 7.0, 7.0, 8.0, 7.0, 4.0, 5.0, 6.0, 10.0, 8.0, 12.0]

channels or external conditions, which may also considerably impact in the MG control stability [42]. Moreover, the infrastructure topology is also an important feature in terms of stability, specially in this kind of application in which variations, connections and disconnections of DGs, as well as communication links failures may occur [43], [44].

All these aforementioned aspects of the communication and related impacts on the system stability have attracted important efforts in consensus studies as special subjects of interest. The maturity in such studies in other areas of knowledge may be one of the rich benefits of applying an well established technique (consensus theory) in a new field (MGs). For further information please refer to [45].

Due to space limitations, the theoretical stability considering all these communication particularities are not covered herein, although they are not neglected in the implementation and results presented in Section V, which covers realistic conditions. Time-delays are applied in the scenarios considered and the protocol is also considered stable in time-varying topology, as long as the listed conditions in the subsection IV-C1 are attained in all possible graphs. The DGs whose communication links are out of the established conditions are set to inject maximum active power and zero reactive power. The DGs which still have a strong connectivity, including the leader node, follow the Consensus-PBC, as exemplified in Subsection V-B3 and V-B4.

V. SIMULATION RESULTS

A. Microgrid Simulated Circuit

The Consensus-PBC is evaluated through time-domain simulation implemented in *Matlab/Simulink* considering the MG of Fig. 2 and the steps described in Section IV. Such circuit is part of a real low-voltage urban distribution power system with the parameters available in [23]. Non-linear (NL) loads are added according to Fig. 2 resulting in a total MG demand of approximately $[36.0\ 38.0\ 32.0]$ *kW* and $[15.0\ 14.0\ 12.0]$ *kvar* in phases $[a\ b\ c]$. The DGs are randomly located and connected arbitrarily either line-to-neutral or line-to-line, which is a real need in Brazilian NTs. The aggregated power rating of DGs are $A_{inv} = [36.33.0\ 36.33\ 37.33]$ *kVA* and $P_{max} = [30.0\ 32.0\ 32.0]$ *kW*. They are modeled as ideal controlled current sources, since the primary control is not the main focus herein. The parameters of DGs are shown in Table I. Apart from the UI, all DGs operate in current-control mode.

TABLE II
OPERATIONAL CONDITIONS CONSIDERED IN THE SIMULATION
CASE 1 - POWER SHARING

Time (s)	Operational conditions
0.35	- GC mode: CB_1 and CB_2 closed, CB_{UI} closed; - Radial topology: CB_3 and CB_4 opened; - All DGs connected: all S_n closed; - $P_G^* = [8.0, 10.0, 12.0]$ kW, $Q_G^* = [4.0, 3.0, 1.0]$ kvar.
0.50	- $P_G^* = [15.0, 15.0, 15.0]$ kW, $Q_G^* = [2.0, 2.0, 2.0]$ kvar.
1.00 1.05 1.10	- Intentional islanding: $P_G^* = [0.0, 0.0, 0.0]$ kW, $Q_G^* = [0.0, 0.0, 0.0]$ kvar; CB_1 opens; CB_2 opens.
1.25	- Meshed topology: CB_3 and CB_4 closes.
1.50	- Load step (connection of NL loads).
2.00 2.05 2.10	- GC mode: CB_2 closes; CB_1 closes; $P_G^* = [15.0, 15.0, 15.0]$ kW, $Q_G^* = [2.0, 2.0, 2.0]$ kvar.

B. Case Studies and Analysis

As detailed in the subsections from V-B1 to V-B5, the case studies cover different realistic operational conditions, such as GC and IS operating modes, as well as the transitions between them, PCC power flow control, unbalance current compensation at PCC, meshed/radial topology, load step variation with non-linear loads, different communication failures, plug-and-play procedure of DGs and communication time-delays. Considering a urban MG with short distances, a time-delay of 1 *ms* is considered in each communication link during the whole simulation in the cases 1, 2 and 3 (*a* and *b*), unless it is stated otherwise as in the specific study of communication time-delays in case 4, where this subject is discussed in detail.

1) Power Sharing Analysis: Fig. 2 shows the initial condition of the breakers in the MG circuit when simulation starts in the Case 1, i.e., GC mode, UI connected, radial topology, linear loads, and all DGs connected and participating in the Consensus-PBC. Fig. 7 shows the simulation results with the x-axis divided in operational conditions according to Table II. For some cases just the results of active power are shown, but the expected behavior was obtained for reactive power, in some places omitted for the sake of space.

In short, Fig. 7 shows the contribution of the main grid and UI to the power sharing, as well as the line and neutral currents ($I_{PCC} = I_G + I_{UI}$) and voltage profile at the PCC. The contribution of DGs is shown by the Consensus-PBC α_P and α_Q, for single- and three-phase DGs.

To characterize the system, details of voltage and current waveforms at the PCC from Fig. 7 are shown in Fig. 8. The results in Fig. 8(a) and (b) were measured before the connection of non-linear loads and the load step in the system at 1.50 *s*, and Fig. 8(c) and (d) afterwards, which is evidenced by the distortions observed in PCC current. Back to Fig. 7, observe that the Consensus-PBC shows a stable operation. All changes applied occurs smoothly.

Fig. 9(a) and 9(b) show how the active and reactive power at PCC are accurately controlled, following the change in the power flow reference at 0.50 *s*. The graph presented in Fig. 9(c) shows the active power sharing of the single-phase DGs connected to phase *a* proportionally to their capacities, as

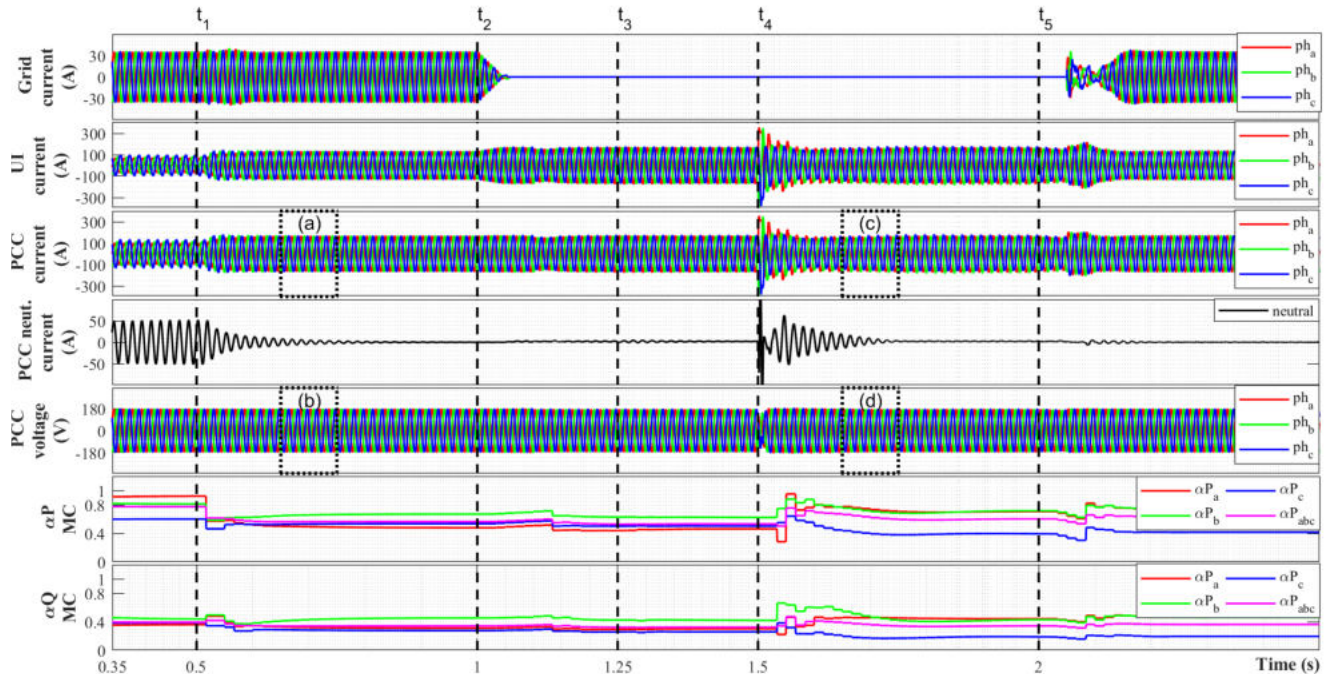

Fig. 7. Simulation results-overview. From top to bottom: grid currents, UI currents, PCC currents, PCC neutral current, PCC voltages, α_P and α_Q, respectively.

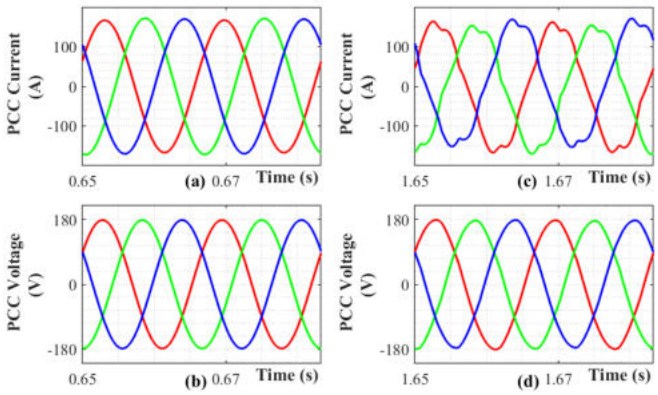

Fig. 8. Current and voltage waveforms: (a) PCC currents and (b) PCC voltages before t_4, (c) PCC currents and (d) PCC voltages after t_4, respectively.

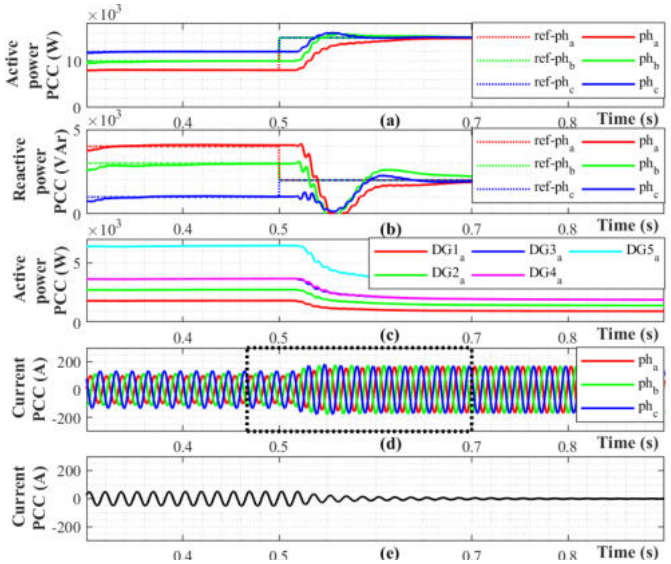

Fig. 9. System behavior under changes in PCC power flow references and unbalance compensation at t_1: (a) PCC active power. (b) PCC reactive power. (c) Convergence of the scaling coefficients for active power of DGs_a. (d) PCC currents. (e) PCC neutral current.

specified in Table I: e.g., $DG3_a$ and $DG4_a$ present the same power rating, thus, they inject the same active power to MG. When a balanced power flow reference is set to PCC at t_1, the unbalance compensation at this node occurs in Fig. 9(d), zoomed in and shown in Fig. 10, which is also evidenced by the reduction of the PCC neutral current in Fig. 9(e).

2) MG Operating Modes: as highlighted by the dashed lines in Fig. 7, the MG experiences different operating modes, as an IS starting at 1.00 *s*, detailed in Fig. 11. The grid and UI currents, as well as the currents at the PCC during this transition, are shown in Fig. 11(a), (b), and (c), respectively. The UI operates as grid-forming converter during all IS mode, providing the necessary voltage reference for the whole MG. At t_5 in Fig. 7, the MG re-connection to the main grid initiates. In both operational modes, as well as during the transitions, the system reacts also smoothly, in a stable and safe condition.

3) Plug-and-Play Capability: herein two different scenarios are considered: *(1)* when the DG is participating in the Consensus-PBC but disconnects from the MG for any reason and re-connects afterwards; and *(2)* when the DG owner has decided not participate in the Consensus-PBC and afterwards changes decision. In both cases it is considered that the communication links are still available and operating. Communication failures are discussed in Section V-B4.

In case *(1)* the disconnected DG_i informs zero availability in step (B) and all other steps are kept the same. This

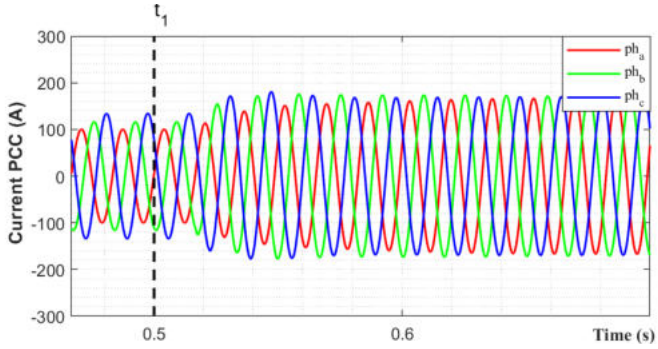

Fig. 10. Details of the current unbalance compensation at PCC started at t_1.

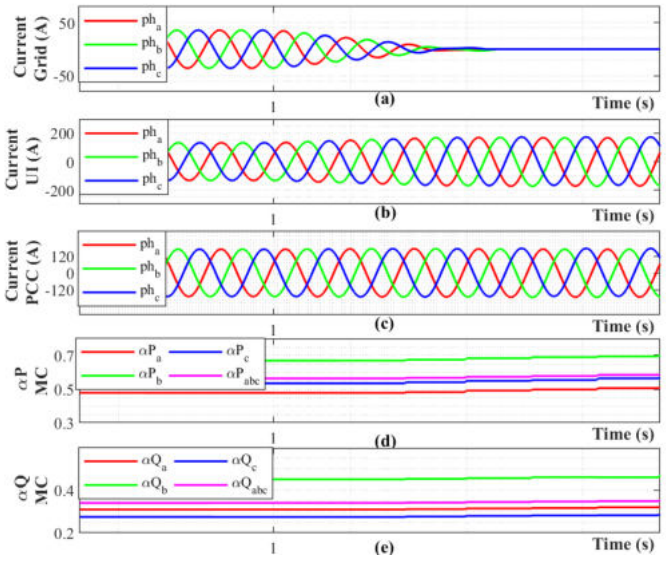

Fig. 11. System behavior during transition from GC mode to IS mode at t_2: (a) Grid currents. (b) UI currents. (c) PCC currents. (d) Scaling coefficient for active power at MC, and (e) for reactive power at MC.

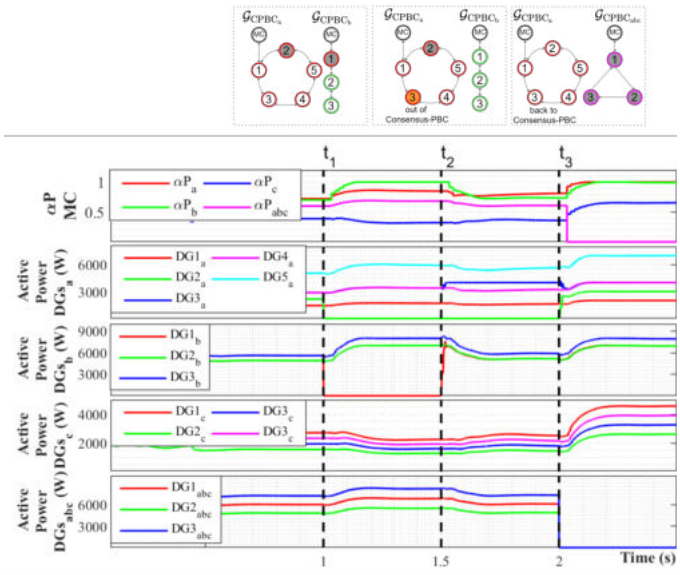

Fig. 12. System behavior during plug-and-play process: (a) Scaling coefficient for active power at MC. (b) Active power shared by DGs connected to phase a, (b) phase b, (c) phase c and, (d) for the three-phase DGs.

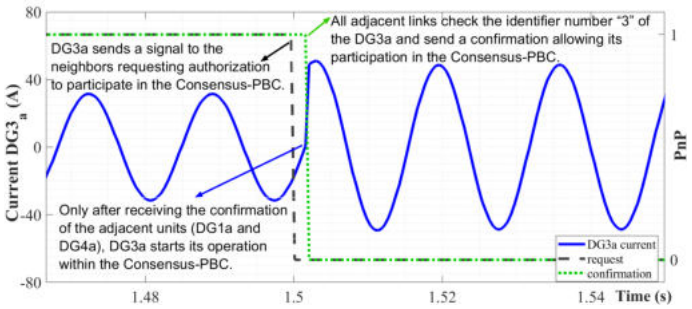

Fig. 13. Plug-and-play procedure for $DG3_a$.

behavior is exemplified when DG_{2_a} disconnects from the system (or does not have available energy) in the interval from 1.00 to 2.00 s and DG_{1_b} from 1.00 to 1.50 s, as shown in Fig 12. In this figure, all scaling coefficient related to active power sharing, in all phases, are shown. When DG_{2_a} and DG_{1_b} disconnects, the scaling coefficient of these phases increases to compensate the loss of power availability with the other DGs still operating. The opposite is observed when these DGs re-connects to the system.

In case *(2)*, in turn, a signal request is sent from the DG to all its adjacent agents when there is any change in its participation decision in the Consensus-PBC, as occurred at 1.50 s for $DG3_a$ in Fig 12. Just when this DG receives the confirmation from all adjacent neighbors, the generation unit is able to participate or leave the power sharing controlled by the Consensus-PBC (see the current change at the same time as the reception of the confirmation in Fig. 13). If the DG does not participate in the Consensus-PBC but is still available and connected to the power system, its generation is set to $\alpha_P = 1$ and $\alpha_Q = 0$. Notice in Fig. 12 how α_P and α_Q react to reestablish the power balance. Still in Fig. 12, when the DG returns at 2.00 s, the scaling coefficients are adapted and the $DG3_a$ starts to follow α_P and α_Q obtained by the Consensus-PBC. Afterwards, when all three-phase DGs disconnect from the system, all single-phase scaling coefficients increases to reestablish the power sharing.

TABLE III
OPERATIONAL CONDITIONS CONSIDERED IN THE SIMULATION CASE 2 - PLUG-AND-PLAY PROCEDURE

Time (s)	Operational conditions
0.35	- IS mode: CB_1 and CB_2 opened, CB_{UI} closed; - Meshed topology: CB_3 and CB_4 closed; - All DGs connected: all S_n closed; - $P^*_G = [0.0, 0.0, 0.0]$ kW $Q^*_G = [0.0, 0.0, 0.0]$ kvar.
1.00	- Disconnection of DG_{2_a} and DG_{1_b}.
1.50	- DG_{3_a} leaves the Consensus-PBC. - Re-connection of DG_{1_b}.
2.00	- DG_{3_a} requests participation in the Consensus-PBC; - Re-connection of DG_{2_a}.

4) Communication Failures: to analyze the system behavior against communication failures, the graphs related to phases *a* and *b* (Fig. 4(a) and (b)) are considered with different topologies. Observe in Fig. 4(a) that, besides being strongly connected, the graph is also cyclic. That means, there is a redundancy link which keeps the graph still strongly connected

TABLE IV
OPERATIONAL CONDITIONS CONSIDERED IN THE SIMULATION
CASE 3 - COMMUNICATION FAILURES

Time (s)	Operational conditions
0.35	- IS mode: same initial condition of Table III.
Case 3a	**Communication failures in DGs at phase *a***
1.00	- Communication failure at link DG_{1_a}-DG_{2_a}.
1.50	- Restoring of link DG_{1_a}-DG_{2_a}, failure at link DG_{3_a}-DG_{4_a}.
2.00	- Restoring of link DG_{3_a}-DG_{4_a}
Case 3b	**Communication failures in DGs at phase *b***
1.00	- Communication failure at link DG_{1_b}-DG_{2_b}.
1.50	- Restoring of link DG_{1_b}-DG_{2_b}, failure at link DG_{2_b}-DG_{3_b}.
2.00	- Restoring of link DG_{2_b}-DG_{3_b}

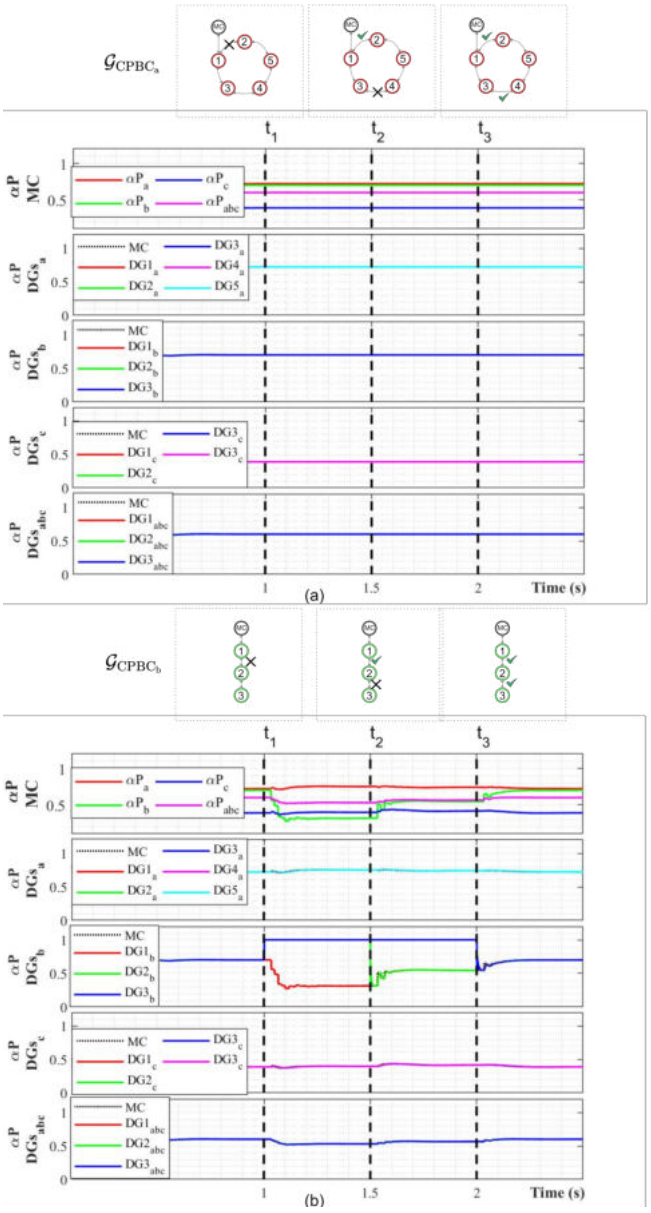

Fig. 14. System behavior during communication failures: (a) in single-phase DGs connected to phase a, (b) in single-phase DGs connected to phase b. From top to bottom: Scaling coefficient for active power at MC, consensus on scaling coefficients for active power in the DGs connected to the phase a, phase b, phase c and, for the three-phase DGs.

even in case of a single failure. This is the first condition simulated in Case 3a, as shown in Fig. 14(a). At 1.00 s a failure at the link DG_{1_a}-DG_{2_a} is applied, and at 1.50 s at the link DG_{3_a}-DG_{4_a}. In both failures, the communication path changes, but the data still reaches the MC at the PCC. This results in no changes in the graphs during this interval.

Analyzing the graph of phase b, it is clear that the condition is different. If any of the links are out of operation, at least one DG would not be reached by all other units and its status would not arrive at the MC. Hence, the DGs out of the SCG connected to the MC are set to inject maximum active power and zero reactive power. The simulation results of Case 3b are presented in Fig. 14(b). At 1.00 s the link DG_{1_b}-DG_{2_b} is interrupted and just the DG_{1_b} is connected to MC. When this link is re-established, a failure occurs between DG_{2_b}-DG_{3_b}, segregating only $DG3_b$. Thus, DG_{2_b} returns to the Consensus-PBC (α_P increases), while-DG_{3_b} keeps injecting maximum active power with unity power factor.

Observe that the total of three-phase DGs is the same as single-phase DGs connected to the phase b. However, only for demonstration a different graph was chosen. In Fig. 4(d) a failure in any link would excludes all DGs not connected directly to the leader from the control coordination. So, a graph as in Fig. 4(b) could be chosen to increase the reliability.

5) Communication Time-Delays: to provide an overview of the system behavior under communication time-delays, different scenarios considering the requirement of 100 ms from IEC 61850 were simulated and are shown in Fig. 15. In each scenario the delay is applied during the whole simulation time, which is more critical than aleatory delays in real applications. As shown in the legend in Fig. 15, the scenario 1 considers a delay of $\tau_1 = 1$ ms in all communication links of the system and in all algorithm steps, scenario 2 a delay of $\tau_2 = 100$ ms in all links during data processing and data transfer from MC to DGs in step (C), and scenario 3 a delay of $\tau_3 = 100$ ms in all links during the consensus protocol in step (D). Finally, in scenario 4 a delay of $\tau_4 = 100$ ms were inserted in some aleatory links in the MG and in different algorithm steps, in order to simulate a more realistic condition. Fig. 15 shows that, despite different convergence times among the scenarios, with exception of scenario 3, similar final values are reached. When all links of the consensus protocol experiences the time-delay of 100 ms the final value diverges from the other scenarios, but keeps still stable. Deeper analysis about this subject is going to be addressed as future work.

VI. COMPARISON WITH THE PREVIOUS WORKS FROM LITERATURE REVIEW

A. *Consensus-PBC* vs *PBC*

Since the control strategy Consensus-PBC is resulted of a combination of the strategy PBC and consensus protocol, Fig. 16(a) and (b) show details of the scaling coefficients calculation in the MC during a change of the PCC power reference for the original PBC, as in [19], and Consensus-PBC, proposed herein. The simulation conditions are described in Table II. Observe that, even with different communication NTs both control strategies present similar results.

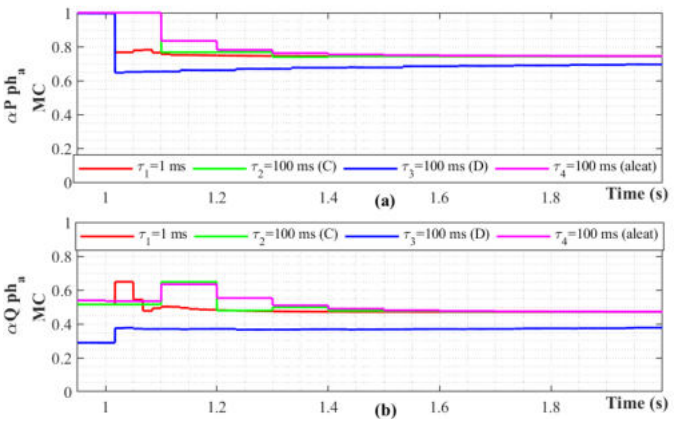

Fig. 15. Scaling coefficients for active power under different communication time delays: $\tau_1 = 1\ ms$, $\tau_2 = 100\ ms$ in step (C), $\tau_3 = 100\ ms$ in step (D), $\tau_4 = 100\ ms$ in aleatory links

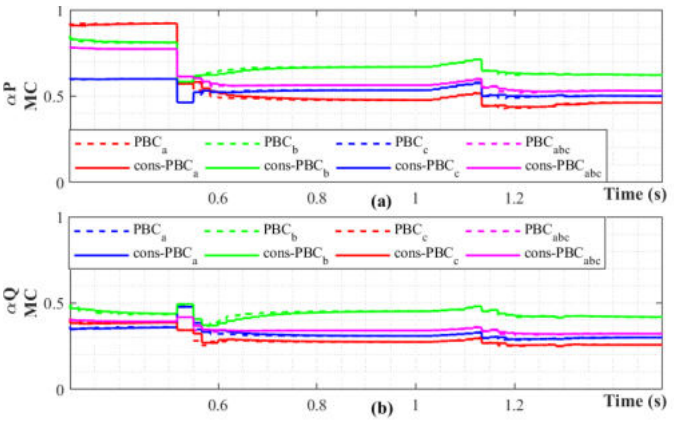

Fig. 16. Scaling coefficient comparison between PBC and Consensus-PBC.

B. *Consensus-PBC* vs *Previous Works*

With different communication technologies available nowadays, there are several ways to promote the information flow through the graphs in Fig. 4. To quantitatively compare in terms of communication NT, however, if it is considered a wired infrastructure and that ICT devices are placed as represented by the graph edges (i.e., communication between the MC and each DG in the centralized approach by an individual wire).

The distances considered are the real values of the system in Fig. 2. In such condition, the total reduction in the wired infrastructure reaches approximately 30 % with the adoption of Consensus-PBC. However, more important than the decrease of the NT is the increase of the flexibility to choose the best communication NT topology with the Consensus-PBC, since the conditions from Subsection IV-C are guaranteed. The graph may be chosen in terms of communication costs, installation complexity, preexisting infrastructure, convergence speed of the protocol or even in terms of reliability (i.e., with the adoption of redundancies as exemplified by the graphs in Fig. 4). Besides the power sharing accuracy and communication approach previously discussed, other features of the control system herein are compared in Fig. 17 with the proposals covered in Section I-A.

In [10], to overcome the trade-off between reactive power sharing and voltage regulation, the techniques/methods average-consensus protocol, leader-follower consensus protocol, droop control, virtual impedance and sequence component analysis are necessary. Even applying all these methods, the control of power flow at PCC is not possible. On the other hand, a recent work published in [16] might be considered one of the most complete proposals among the references herein, offering many benefits to the control systems of MGs. However, many techniques also have to be combined, detailed dynamic and non-linearity are involved and parameters tuning is necessary, increasing the implementation complexity of the control system. Comparing all other previous works herein covered, the low complexity of the Consensus-PBC here proposed may be considered one of its main benefits for the MG development.

One particular feature in this proposal is also obtained by the step (B) in Fig. 5 and Fig. 6. In the end of the information exchange convergence all DGs have the whole information regarding the main quantities for the step (C). If any DG receives the measurements from the grid, UI and power flow references (which could be sent also by the same methodology as in (B)), the step (C), data processing, may be performed in any DG_i. The algorithm involved is simple and does not have special requirements. That means, creating some strategical redundancies to send the mentioned measurements to more than one DG, these DGs could assume the role of leaders, increasing the system reliability considerably in case of leader failures or MC failures, using the existing converters. For the sake of space, this topic is going to be addressed in further works, as well as the data packet loss.

Other point to be highlighted is regarding the operational conditions commonly covered in the papers from literature review. Many of them do not present results or even discussions covering important realistic conditions in MGs. The behavior of the system under communication failures, as well as the plug-and-play process are neglected in [20]. In general, the results are presented mostly through simulations in small NTs. Few proposals addresses different connections of singe-phase DGs coexisting with three-phase DGs.

In this way, an assessment of each work covered in the literature review is conducted in this section. The summary presented in Fig. 18 is based on the parameters adopted and presented in the figure caption. The control system is considered with high complexity if it presents at least two of the elements enumerated; medium for one, and low if any feature above is observed. High limitations regarding the reliability means that the proposal does not present any tolerance or alternatives to deal with two or more characteristics listed; medium for one, and low if the control is able to deal with all scenarios considered. For the limitations to choose communication NT, high is in case of (1) or (2), medium (3) and low (4) or (5). Finally, the manuscript explores or not the flexibility in the communication topology choice based on the project priorities, e.g., cost reduction, communication reduction, reliability improvement, etc. The colors red, yellow and green are just a way to highlight these selected features as high, medium or low, respectively.

	MAIN FEATURES	REFERENCES																
		[5]	[6]	[7]	[8]	[9]	[10]	[11]	[12]	[13]	[14]	[15]	[16]	[17]	[18]	[19]	[20]	THIS PAPER
		2015	2015	2015	2016	2017	2018	2018	2018	2018	2019	2019	2019	2018	2018	2019	2019	2020
IMPLEMENTATION FEATURES AND RESULTS	**Consensus protocol**	- average consensus	- weighted average consensus - leader-follower consensus	- weighted average consensus	- weighted average consensus	- leader-follower consensus	- average consensus - leader-follower consensus	- leader-follower consensus	- leader-follower consensus	- average consensus	- weighted average consensus	leader-follower consensus	- average consensus - leader-follower consensus	-	-	-	-	- leader-follower consensus
	Dynamic model: high-order dynamics, non-linearities or linearization techniques?	no	yes	yes	no	yes	yes	yes	yes	no	yes	yes	yes	-	-	no	-	no
	Other techniques	- cost optimization - load shedding	- droop control	- frequency droop control	- droop control - virtual impedance	-	- droop control - virtual impedance - sequence component analysis	- droop control	- droop control - stave observer	- primal-dual constrained decomposition theory - droop control	-others	- droop control - virtual impedance	- droop control - virtual impedance	- frequency droop control	- droop control - conservative power theory - unbalanced virtual output impedance - opitimazation problem	- power-based control	- droop control	- power-based control
	Coordinate transformation	no	no	no	abc - αβ	abc - dq	abc - αβ	abc - αβ	-	-	abc - dq	no	no	αβ - abc	abc - αβ	no	abc - αβ	no
	Hierarchical architecture (yes, no) (level of the consensus protocols)	yes (1º)	yes (2º)	no	yes (2º)	no	yes (1º, 2º)	yes (2º)	yes (2º)	yes (2º, 3º)	yes (1º, 2º)	yes (2º)	yes (2º, 3º)	yes (-)	yes (-)	yes (-)	yes (-)	yes (2º)
	Master controller (yes, no)	no	no	no	no	no	no	no	no	no	no	no	no	yes	yes	yes	no	yes
	Leader node (yes, no) (fixed, flexible)	no	no/yes fixed	no	no	yes fixed	yes fixed	yes fixed	yes fixed	no	no	yes fixed	yes fixed	no	no	-	no	yes flexible
	Communication topology (directed balanced, directed unbalanced, undirected)	directed unbalanced (SCG)	undirected (SCG)	undirected (SCG)	undirected (SCG)	undirected (SCG)	directed (SCG)	undirected (SCG)	undirected (SCG)	directed unbalanced (SCG)	without details	undirected (SCG)	undirected (SCG)	undirected / centralized	undirected / centralised	undirected / centralised	without comm.	connected (SCG)
	Time delay (yes, no) (delay in *ms*)	yes -	yes -	no -	yes 31.4	no -	no -	no -	yes 5	no -	no	yes 100, 300, 400	yes 30, 100, 300	no -	no -	yes 167	without comm.	yes 1 - 100 ms
	Network features (voltage level) (frequency) (single-phase (1Φ), three-phase (3Φ)) (3-wire or 4-wire if 3Φ) (radial, meshed) (# Nodes) (# Agents (controllable units))	400 V 50 Hz 3Φ 4-wire radial 19 nodes 5 agents	230 V 50 Hz 1Φ - radial 4 nodes 4 agents	20 kV 50 Hz 3Φ - meshed 11 nodes 6 agents	120 V 50 - 60 Hz 3Φ 3-wire radial 4 nodes 4 agents	400 V 50 Hz 3Φ 4-wire radial 8 nodes 10 agents	4.16 kV 60 Hz 3Φ 3-wire radial 13 nodes 4 agents	311 V 50 Hz 1Φ - radial 4 nodes 4 agents	220 V 50 Hz 1Φ - radial 33 nodes 6 agents	- 60 Hz 3Φ 3-wire radial 25 nodes 5 agents	- 60 Hz 3Φ - meshed 6 nodes 6 agents	- - 1Φ - radial 4 nodes 4 agents	- - 3Φ radial 4-wire - 4 MGs	- 60 Hz 3Φ 3-wire - 1 node per phase 1 agent per phase	180 V - 3Φ 4-wire radial 2 nodes 2 agents	220 V 60 Hz 3Φ 3-wire radial 13 nodes 6 agents	100 V 50 Hz 3Φ 4-wire radial 2 nodes 2 agents	127 V 60 Hz 3Φ 4-wire radial / meshed 43 nodes 15 agents (12 1Φ, 3 3Φ)
	DGs features (1Φ, 3Φ) (VCM,CCM) (P-Q control, V-f control) (power rating kVA) (power rating kW)	3Φ - P-Q, V-f 30.0-100.0 10.0-100.0	1Φ - V-f 0.8-1.6 0.7-1.4	1Φ VCM V-f control '- '-	3Φ VCM V-f control - 20.0	1Φ | 3Φ - P-Q 10.0 10.0	- VCM V-f - ratio 1:2:3:4	1Φ - V-f - -	1Φ - V-f - 2.0-13.0	3Φ - V-f, P-f - -	3Φ - V-f - -	1Φ - V-I control - -	1Φ | 3Φ VCM V-f control - -	1Φ - V-f - 1.0	3Φ - V-f - 5.0	1Φ | 3Φ VCM, CCM P-Q 5.0-33.0 4.5-22.5	3Φ VCM V-f control - 3.0	1Φ | 3Φ CCM, VCM P-Q control, V-f control 3.0-9.0 | 10.0-14.0 2.0-8.0 | 8.0-12.0
	Type of results available (software, HIL, experimental results)	software (PSCAD/EMTDC/Matlab/PSCAD)	- software (Simulink) - experimental	- software (Plecs)	- software (Matlab/ Simulink) - experimental	- software (Matlab/ Simulink)	- software (Matlab/ Simulink)	- software (time-domain simulations)	- software (Matlab/ Simulink)	- software	- software (Matlab/ Simulink)	- software (Matlab/ Simulink)	- software (Matlab/ Simulink)	- software (PSCAD/ EMTDC)	- software (Plexim PLECS) - experimental	- software - experimental	- software (PLECS) - experimental	- software (Matlab/ Simulink)
	Analysis method (profile of the quantities, indices application, stability analysis)	profile stability analysis	- profile	- profile - stability analysis	- profile	- profile - indices	- profile	- profile - stability analysis	- profile - stability analysis	- profile - stability analysis - indices	- profile - stability analysis - indices	- profile	- profile	- profile	- profile - indices	- profile	- profile - indices	- profile - stability analysis

Fig. 17. Main features of control systems from literature of interest to the Consensus-PBC.

VII. Conclusion

A distributed control strategy for MG was proposed combining the advantages of the centralized power-based control (PBC) strategy and the distributed technique leader-following consensus protocol. In the proposed Consensus-PBC the information flows in a distributed communication infrastructure. The central converter and master controller from the PBC are kept. A adapted real low-voltage distribution system was simulated in several operational conditions.

The proposed technique provided stable and accurate power sharing among DGs, tight power flow control and current unbalance compensation at the PCC, not only under normal operation as well as during undesired scenarios. Besides the benefits to the NT, this manuscript also contributes providing a simple theoretical understanding of the stability in leader-follower consensus protocols in discrete-time. The combination of consensus protocol with the PBC implies in a model-free approach as well as no need of details from the primary control dynamic, resulting in a system with low calculation complexity in comparison with other applications found in the literature. The sparse communication NT leads to improved system scalability, flexibility of communication topology design, cost reduction, and improvement of the system reliability, all important features for the future growth of the MG technology.

For enhancement of the proposed method some future works are planned: detailed modeling and analysis of communication restrictions and disturbances, inclusion of new scenarios in the implementation, and application of quality and performance indices for a quantitative evaluation of the strategy proposed.

Acknowledgment

This project was funded by the Brazilian agencies CAPES, CNPq, FAPEMIG, and by Petróleo Brasileiro (Petrobras) under Agência Nacional de Energia Elétrica (ANEEL) Research Grant PD-00553-0046/2016, and also by the Norwegian institution Research Council of Norway under Grant f261735/H30. Additionally, the authors thank the Norwegian University of Science and Technology for all support given to this project.

References

[1] A. Hirsch, Y. Parag, and J. Guerrero, "Microgrids: A review of technologies, key drivers, and outstanding issues," *Renewable and Sustainable Energy Reviews*, vol. 90, no. April, pp. 402–411, 7 2018.

[2] T. Morstyn, B. Hredzak, and V. G. Agelidis, "Control Strategies for Microgrids With Distributed Energy Storage Systems: An Overview," *IEEE Transactions on Smart Grid*, vol. 9, no. 4, pp. 3652–3666, 7 2018.

[3] K. Manjunath and V. Sarkar, "Performance assessment of different droop control techniques in an AC microgrid," *2017 7th International Conference on Power Systems, ICPS 2017*, pp. 93–98, 2018.

[4] R. Hidalgo-León, C. Sanchez-Zurita, P. Jácome-Ruiz, J. Wu, and Y. Muñoz-Jadan, "Roles, challenges, and approaches of droop control methods for microgrids," *2017 IEEE PES Innovative Smart Grid Technologies Conference - Latin America, ISGT Latin America 2017*, vol. 2017-Janua, pp. 1–6, 2017.

[5] W. Liu, W. Gu, Y. Xu, S. Xue, M. Chen, B. Zhao, and M. Fan, "Improved average consensus algorithm based distributed cost optimization for loading shedding of autonomous microgrids," *International Journal of Electrical Power and Energy Systems*, vol. 73, pp. 89–96, 2015.

[6] J. W. Simpson-Porco, Q. Shafiee, F. Dorfler, J. C. Vasquez, J. M. Guerrero, and F. Bullo, "Secondary Frequency and Voltage Control of Islanded Microgrids via Distributed Averaging," *IEEE Transactions on Industrial Electronics*, vol. 62, no. 11, pp. 7025–7038, 11 2015.

[7] J. Schiffer, T. Seel, J. Raisch, and T. Sezi, "Voltage Stability and Reactive Power Sharing in Inverter-Based Microgrids With Consensus-Based Distributed Voltage Control," *IEEE Transactions on Control Systems Technology*, vol. 24, no. 1, pp. 96–109, 1 2016.

[8] J. Zhou, S. Kim, H. Zhang, Q. Sun, and R. Han, "Consensus-Based Distributed Control for Accurate Reactive, Harmonic, and Imbalance Power Sharing in Microgrids," *IEEE Transactions on Smart Grid*, vol. 9, no. 4, pp. 2453–2467, 7 2018.

[9] C. Huang, S. Weng, D. Yue, S. Deng, J. Xie, and H. Ge, "Distributed cooperative control of energy storage units in microgrid based on multi-agent consensus method," *Electric Power Systems Research*, vol. 147, pp. 213–223, 6 2017.

[10] L. Yu, D. Shi, G. Xu, X. Guo, Z. Jiang, and C. Jing, "Consensus Control of Distributed Energy Resources in a Multi-Bus Microgrid for Reactive Power Sharing and Voltage Control," *Energies*, vol. 11, no. 10, p. 2710, 10 2018.

[11] X. Hou, Y. Sun, J. Lu, X. Zhang, L. H. Koh, M. Su, and J. M. Guerrero, "Distributed hierarchical control of AC microgrid operating in grid-connected, islanded and their transition modes," *IEEE Access*, vol. 6, pp. 77 388–77 401, 2018.

[12] L. Chen, Y. Wang, X. Lu, T. Zheng, J. Wang, and S. Mei, "Resilient Active Power Sharing in Autonomous Microgrids Using Pinning-Consensus-Based Distributed Control," *IEEE Transactions on Smart Grid*, vol. PP, no. c, pp. 1–1, 2019.

[13] P. P. Vergara, J. M. Rey, H. R. Shaker, J. M. Guerrero, B. N. Jorgensen, and L. C. P. da Silva, "Distributed Strategy for Optimal Dispatch of Unbalanced Three-Phase Islanded Microgrids," *IEEE Transactions on Smart Grid*, vol. 10, no. 3, pp. 3210–3225, 5 2019.

[14] J. Duan, C. Wang, H. Xu, W. Liu, Y. Xue, J.-c. Peng, and H. Jiang, "Distributed Control of Inverter-Interfaced Microgrids Based on Consensus Algorithm With Improved Transient Performance," *IEEE Transactions on Smart Grid*, vol. 10, no. 2, pp. 1303–1312, 3 2019.

[15] J. Zhou, Y. Xu, H. Sun, L. Wang, and M.-Y. Chow, "Distributed Event-Triggered H_∞ Consensus Based Current Sharing Control of DC Microgrids Considering Uncertainties," *IEEE Transactions on Industrial Informatics*, vol. XX, no. XX, pp. 1–1, 2019.

[16] J. Zhou, Y. Xu, H. Sun, Y. Li, and M. Y. Chow, "Distributed Power Management for Networked AC-DC Microgrids with Unbalanced Microgrids," *IEEE Transactions on Industrial Informatics*, vol. 16, no. 3, pp. 1655–1667, 2020.

[17] S. A. Raza and J. Jiang, "Intra-and Inter-Phase Power Management and Control of a Residential Microgrid at the Distribution Level," *IEEE Transactions on Smart Grid*, vol. 10, no. 6, pp. 6839–6848, 2019.

[18] C. Burgos-Mellado, R. Cardenas, D. Saez, A. Costabeber, and M. Sumner, "A Control Algorithm Based on the Conservative Power Theory for Cooperative Sharing of Imbalances in Four-Wire Systems," *IEEE Transactions on Power Electronics*, vol. 34, no. 6, pp. 5325–5339, 2019.

[19] D. I. Brandao, L. S. Araujo, A. M. S. Alonso, G. L. dos Reis, E. V. Liberado, and F. P. Marafao, "Coordinated Control of Distributed Three-and Single-phase Inverters Connected to Three-Phase Three-Wire Microgrids," *IEEE Journal of Emerging and Selected Topics in Power Electronics*, vol. PP, no. c, pp. 1–1, 2019.

[20] E. Espina, R. Cardenas-Dobson, M. Espinoza-B., C. Burgos-Mellado, and D. Saez, "Cooperative Regulation of Imbalances in Three-Phase Four-Wire Microgrids Using Single-Phase Droop Control and Secondary Control Algorithms," *IEEE Transactions on Power Electronics*, vol. 35, no. 2, pp. 1978–1992, 2 2020.

[21] T. Caldognetto, S. Buso, P. Tenti, and D. I. Brandao, "Power-Based Control of Low-Voltage Microgrids," *IEEE Journal of Emerging and Selected Topics in Power Electronics*, vol. 3, no. 4, pp. 1056–1066, 12 2015.

[22] D. I. Brandao, T. Caldognetto, F. P. Marafao, M. G. Simoes, J. A. Pomilio, and P. Tenti, "Centralized Control of Distributed Single-Phase Inverters Arbitrarily Connected to Three-Phase Four-Wire Microgrids," *IEEE Transactions on Smart Grid*, vol. 8, no. 1, pp. 437–446, 1 2017.

[23] D. I. Brandao, L. S. de Araújo, T. Caldognetto, and J. A. Pomilio, "Coordinated control of three- and single-phase inverters coexisting in low-voltage microgrids," *Applied Energy*, vol. 228, no. March, pp. 2050–2060, 10 2018.

[24] T. Caldognetto, P. Tenti, A. Costabeber, and P. Mattavelli, "Improving microgrid performance by cooperative control of distributed energy sources," *IEEE Transactions on Industry Applications*, vol. 50, no. 6, pp. 3921–3930, 2014.

[25] H. Zhang, F. L. Lewis, and Z. Qu, "Lyapunov, Adaptive, and Optimal Design Techniques for Cooperative Systems on Directed Communication Graphs," *IEEE Transactions on Industrial Electronics*, vol. 59, no. 7, pp. 3026–3041, 7 2012.

MAIN FEATURES		REFERENCES																
		[5]	[6]	[7]	[8]	[9]	[10]	[11]	[12]	[13]	[14]	[15]	[16]	[17]	[18]	[19]	[20]	THIS PAPER
		2015	2015	2015	2016	2017	2018	2018	2018	2018	2019	2019	2019	2018	2018	2019	2019	2020
EVALUATION	Implementation complexity	high (3, 4)	high (1, 2, 3)	high (1, 2, 3)	high (1, 3, 6)	high (1, 3, 6)	high (1, 3, 6)	high (1, 2, 3, 6)	high (1, 3)	high (3, 4)	high (1, 3, 6)	high (1, 3)	high (1, 2, 3)	medium (3, 6)	high (3, 4, 6)	low	high (1, 3)	low
	Limitations concerning reliability	high (1, 2)	medium (4)	medium (1, 2)	low	medium (4)	medium (3, 4)	medium (4)	medium (3, 4)	medium (4)	high (1, 2, 4)	medium (3)	low	high (1, 2, 4)	high (1, 2, 4)	medium (3)	low	medium (3)
	Limitations to choose communication NT	medium (3)	medium (3)	medium (3)	medium (3)	medium (3)	medium (3)	medium (3)	medium (3)	medium (3)	medium (3)	medium (3)	medium (3)	medium (3)	high (2)	high (2)	low (4)	medium (3)
	Project flexibility	no	yes	no	yes	no	no	no	no	yes	no	no	no	no	no	no	no	yes

Fig. 18. Comparative summary of the literature review - Assessment. Parameters considered: a) Implementation complexity: *1)* detailed dynamic; *2)* non-linearity; *3)* parameters tuning; *4)* optimization method; *5)* need of NT parameters; *6)* coordinate transformation. b) Limitations concerning reliability: *1)* agent failure; *2)* communication failure; *3)* dependence on a single DG or MC; *4)* communication time-delay. c) Limitations to choose communication NT (graph characteristics): *1)* specific graph; *2)* centralized; *3)* SCG; *4)* weakly connected graph (WGC); *5)* without communication. d) Project flexibility: yes or no.

[26] R. Olfati-Saber, J. A. Fax, and R. M. Murray, "Consensus and Cooperation in Networked Multi-Agent Systems," *Proceedings of the IEEE*, vol. 95, no. 1, pp. 215–233, 1 2007.

[27] S. Lissandron and P. Mattavelli, "A controller for the smooth transition from grid-connected to autonomous operation mode," *2014 IEEE Energy Conversion Congress and Exposition, ECCE 2014*, pp. 4298–4305, 2014.

[28] S. Buso, T. Caldognetto, and Q. Liu, "Analysis and Experimental Characterization of a Large-Bandwidth Triple-Loop Controller for Grid-Tied Inverters," *IEEE Transactions on Power Electronics*, vol. 34, no. 2, pp. 1936–1949, 2019.

[29] S. M. Ismael, S. H. Abdel Aleem, A. Y. Abdelaziz, and A. F. Zobaa, "State-of-the-art of hosting capacity in modern power systems with distributed generation," *Renewable Energy*, vol. 130, pp. 1002–1020, 1 2019.

[30] O. Slučiak, "Convergence Analysis of Distributed Consensus Algorithms," Ph.D. dissertation, Technischen Universität Wien, 2013.

[31] R. S. Varga, *Gersgorin and His Circles*, ser. Springer Series in Computational Mathematics. Springer Berlin Heidelberg, 2004, vol. 8.

[32] R. B. Bapat and T. E. S. Raghavan, *Perron-Frobenius theory and matrix games*. Cambridge University Press, 2009.

[33] D. Serre, *Matrices Theory and Applications*, ser. Graduate Texts in Mathematics. Springer New York, 2010, vol. 216, no. 2.

[34] R. A. Horn and C. R. Johnson, *Matrix Analysis*. Cambridge University Press, 12 1985.

[35] Y. Zheng, S. Li, and R. Tan, "Distributed Model Predictive Control for On-Connected Microgrid Power Management," *IEEE Transactions on Control Systems Technology*, vol. 26, no. 3, pp. 1028–1039, 5 2018.

[36] S. Marzal, R. Salas, R. González-Medina, G. Garcerá, and E. Figueres, "Current challenges and future trends in the field of communication architectures for microgrids," *Renewable and Sustainable Energy Reviews*, vol. 82, no. October 2016, pp. 3610–3622, 2018.

[37] L. Tightiz, H. Yang, and M. J. Piran, "A Survey on Enhanced Smart Micro-Grid Management System with Modern Wireless Technology Contribution," *Energies*, vol. 13, no. 9, p. 2258, 5 2020.

[38] IEEE, "IEEE Standard for Interconnection and Interoperability of Distributed Energy Resources with Associated Electric Power Systems Interfaces," pp. 1–138, 2018.

[39] J. Chen, S. Yan, T. Yang, S.-C. Tan, and S. Y. Hui, "Practical Evaluation of Droop and Consensus Control of Distributed Electric Springs for Both Voltage and Frequency Regulation in Microgrid," *IEEE Transactions on Power Electronics*, vol. 34, no. 7, pp. 6947–6959, 7 2019.

[40] J. Lai, X. Lu, X. Yu, W. Yao, J. Wen, and S. Cheng, "Distributed multi-DER cooperative control for master-slave-organized microgrid networks with limited communication bandwidth," *IEEE Transactions on Industrial Informatics*, vol. 15, no. 6, pp. 3443–3456, 2019.

[41] J. Lai, X. Lu, X. Yu, and A. Monti, "Stochastic Distributed Secondary Control for AC Microgrids via Event-Triggered Communication," *IEEE Transactions on Smart Grid*, vol. 11, no. 4, pp. 2746–2759, 2020.

[42] M. A. Shahab, S. B. Mozafari, S. Soleymani, N. Mahdian, H. Mohammadnezhad, and J. M. Guerrero, "Stochastic Consensus-based Control of μGs with Communication Delays and Noises," *IEEE Transactions on Power Systems*, vol. 8950, no. c, pp. 1–1, 2019.

[43] H. J. Savino, C. R. Dos Santos, F. O. Souza, L. C. Pimenta, M. De Oliveira, and R. M. Palhares, "Conditions for Consensus of Multi-Agent Systems with Time-Delays and Uncertain Switching Topology," *IEEE Transactions on Industrial Electronics*, vol. 63, no. 2, pp. 1258–1267, 2016.

[44] S. Liang, Z. Liu, and Z. Chen, "Leader-following Exponential Consensus of Discrete-time Multi-agent Systems with Time-varying Delay and Intermittent Communication," *International Journal of Control, Automation and Systems*, vol. 17, no. 61573200, pp. 1–11, 2019.

[45] R. Olfati-Saber and R. Murray, "Consensus Problems in Networks of Agents With Switching Topology and Time-Delays," *IEEE Transactions on Automatic Control*, vol. 49, no. 9, pp. 1520–1533, 9 2004.

Daniele M. Ferreira is currently a PhD Candidate in Electrical Engineering with the Federal University of Minas Gerais (UFMG), Belo Horizonte, Brazil. From 2019 to 2020, part of her PhD project was developed at the Norwegian University of Science and Technology (NTNU), Trondheim, Norway. She received her M.Sc. degree from the Federal Center for Technological Education of Minas Gerais (CEFET-MG), Belo Horizonte, Brazil. She graduated in Industrial Electrical Engineering (with honors) from CEFET-MG in 2010, after one year of an international exchange at Karlsruhe University of Applied Sciences (HsKA), Karlsruhe, Germany. She had different work experiences (technical and management oriented) at companies like Vallourec Tubos do Brasil S.A., Brazil, Fraunhofer Institute for Solar Energy Systems (ISE), Germany, and Bosch, at Brazilian, German and Turkish sites. Her research interests are directed to microgrids and renewable energy generation.

Danilo I. Brandão (S'14–M'16) received the Ph.D. degree in electrical engineering from the University of Campinas, Brazil, in 2015. He was a visiting scholar at the Colorado School of Mines, USA, in 2009 and 2013, a visiting scholar at the University of Padova, Italy, in 2014, and a guest professor at the Norwegian University of Science and Technology, Norway, in 2018 and 2020. He is currently an assistant professor at the Graduate Program in Electrical Engineering with the Federal University of Minas Gerais, Belo Horizonte, Brazil. His main research interests are control of grid-tied converters and microgrids. He is a member of SOBRAEP.

Gilbert Bergna-Diaz (S'11–M'19) received a degree in Electrical Power Engineering from the Universidad Simón Bolívar, Caracas, Venezuela, in 2008, a Research Master degree in Electrical Energy from the École Supérieure d'Électricité (Supélec), Paris, France, in 2010, and a joint Ph.D. degree in Electric Power Engineering from the École CentraleSupélec, Paris, and the Norwegian University of Science and Technology (NTNU), Trondheim, Norway, in 2015. In 2014, he joined SINTEF Energy Research, Trondheim, as a Research Scientist, where he was involved in modeling, analysis, and control of high-voltage direct current (HVDC) transmission systems. In 2016, he joined NTNU as a Post-Doctoral Research Fellow working on nonlinear modelling and control of multiterminal HVDC grids. Since 2019, he has been an Associated Professor at NTNU in control of power electronics systems.

Elisabetta Tedeschi received the M.Sc. degree (with honors) in electrical engineering and the Ph.D. degree in industrial engineering from the University of Padova, Italy, in 2005 and 2009, respectively. From 2009 to 2011, she was a post doc researcher at the Norwegian University of Science and Technology (NTNU), working on the grid integration of offshore renewable energies. Having received a Marie Curie Fellowship, she was a Researcher at Tecnalia, Spain, from 2011 to 2013, where she worked as a principal investigator in the FP7-Sea2grid Project, related to the storage needs for the grid integration of wave energy converters. From 2013 to 2014, she was Research Scientist at SINTEF Energy and Adjunct Associate Professor at NTNU. In 2014, she became Full Professor within offshore grid at NTNU. Since 2020 she is also Full professor at the Department of Industrial Engineering of the University of Trento, Italy. She has a core competence in the design and control of energy conversion and transmission and distribution systems, with focus on offshore energy, and power-quality issues. She has led and/or contributed to more than 15 national and international scientific projects and she is the author or co-author of 2 book chapters and more than 100 journals and conference papers in the field of marine energy and energy conversion systems.

Sidelmo M. Silva graduated in Electrical Engineering (with a gold medal for the highest GPA), and received the Master's and Doctoral degrees in Electrical Engineering, from the Federal University of Minas Gerais (UFMG), Brazil, in 1997, 1999, and 2003, respectively. From October 2001 to August 2002, he was in the Development Department of ABB Switzerland, Turgi, as a System and Controls Engineer. From August 2017 to July 2018, Prof. Sidelmo was a visiting Professor at the University of Wisconsin-Madison, USA, where he worked with microgrids. Sidelmo M. Silva is currently an Associate Professor at the Department of Electrical Engineering of the Federal University of Minas Gerais. His research interests include power quality, applications of power electronics in electric power systems, microgrids and renewable energy generation.